Neural Networks 143 (2021) 452–474

Contents lists available at ScienceDirect

Neural Networks

journal homepage: www.elsevier.com/locate/neunet

On the characterization of cognitive tasks using activity-specific short-lived synchronization between electroencephalography channels

B. Orkan Olcay [a,*], Murat Özgören [b], Bilge Karaçalı [a]

[a] Department of Electrical and Electronics Engineering, Izmir Institute of Technology, 35430, Urla, Izmir, Turkey
[b] Department of Biophysics, Faculty of Medicine, Near East University, 99138, Nicosia, Cyprus

ARTICLE INFO

Article history:
Received 12 February 2021
Received in revised form 4 May 2021
Accepted 18 June 2021
Available online 30 June 2021

Keywords:
EEG
Short-lived synchronization
Motor imagery activity characterization
Systematic timing organization
Synchronization measures

ABSTRACT

Accurate characterization of brain activity during a cognitive task is challenging due to the dynamically changing and the complex nature of the brain. The majority of the proposed approaches assume stationarity in brain activity and disregard the systematic timing organization among brain regions during cognitive tasks. In this study, we propose a novel cognitive activity recognition method that captures the activity-specific timing parameters from training data that elicits maximal average short-lived pairwise synchronization between electroencephalography signals. We evaluated the characterization power of the activity-specific timing parameter triplets in a motor imagery activity recognition framework. The activity-specific timing parameter triplets consist of latency of the maximally synchronized signal segments from activity onset Δt, the time lag between maximally synchronized signal segments τ, and the duration of the maximally synchronized signal segments w. We used cosine-based similarity, wavelet bi-coherence, phase-locking value, phase coherence value, linearized mutual information, and cross-correntropy to calculate the channel synchronizations at the specific timing parameters. Recognition performances as well as statistical analyses on both BCI Competition-III dataset IVa and PhysioNet Motor Movement/Imagery dataset, indicate that the inter-channel short-lived synchronization calculated using activity-specific timing parameter triplets elicit significantly distinct synchronization profiles for different motor imagery tasks and can thus reliably be used for cognitive task recognition purposes.

1. Introduction

Analysis of the brain activity patterns associated with cognitive as well as other tasks has become a popular research area for the neuroscience community (Tirsch et al., 2004). Among the handful of cognitive tasks, motor imagery is arguably one of the most remarkable and interesting, even referred to as "embodied cognition" to study brain functioning (Hanakawa, 2016; Höller et al., 2013). Motor imagery, in general, is defined as the mental representation of the covert actions without any external effort (Xu et al., 2014). The neural correlates of different kinds of motor imagery activities were investigated and found to share a similar neural substrate as well as a control mechanism with actual motor execution (Halder et al., 2011; Izumi et al., 1995; Kilintari et al., 2016). Based on these findings, motor imagery tasks have been explored for neurorehabilitation (Chaudhary et al., 2016; Korostenskaja et al., 2017; Lu et al., 2020), sports training (Guillot et al., 2013), skill acquisition (Kraeutner et al., 2014), brain–computer interfaces (BCI) (Park et al., 2013; Schalk et al., 2004; Wolpaw et al., 2002; Yuan & He, 2014) and virtual environment navigation (Pfurtscheller et al., 2006).

Numerous electroencephalography (EEG)-based motor imagery activity recognition studies have been proposed to extract relevant features of the signals collected during motor imagery tasks (Kevric & Subasi, 2017; Wierzgała et al., 2018). To this end, time series modeling (Arnold et al., 1998; Burke et al., 2005; Samdin et al., 2017; Schlögl, 2000), spatial filtering (Blankertz et al., 2008; Lemm et al., 2005; Lotte & Guan, 2011; Ramoser et al., 2000; Song & Epps, 2007; Zhang et al., 2015), time–frequency analysis (Dodia et al., 2019; Hramov et al., 2019; Hsu & Sun, 2009; Ince et al., 2007), scalp voltage topography (Tzovara et al., 2012), entropy-based modeling (Gao et al., 2013; Göksu, 2018; Kee et al., 2017) as well as other methods have been used in previous motor imagery-based brain–computer interface frameworks (Abiri et al., 2019; Bashashati et al., 2007; Dornhege et al., 2004). These methods, in general, aim to characterize the localized brain dynamics extracted from the electrical activities collected via electrodes placed on a specific region of the scalp.

* Corresponding author.
E-mail addresses: bilalolcay@iyte.edu.tr (B. Orkan Olcay), murat.ozgoren@neu.edu.tr (M. Özgören), bilge@iyte.edu.tr (B. Karaçalı).

https://doi.org/10.1016/j.neunet.2021.06.022
0893-6080/

However, it is also known that the brain is organized as a complex network in which the neural information is continuously processed and transferred between different regions of the brain (Jin et al., 2012; Sporns et al., 2004; Stam & Van Dijk, 2002). Distinct regions that take part in this complex network are in continuous interaction with each other functionally in a nonlinear as well as dynamic fashion (Marinazzo et al., 2011; Rubinov & Sporns, 2010; Sporns et al., 2000).

Two types of statistical interactions, also termed statistical connectivity, have been proposed to take place between brain regions (Fingelkurts et al., 2005; Stam & van Straaten, 2012). Functional connectivity refers to the temporal synchronization and effective connectivity refers to the causal synchronization between the electrophysiological/hemodynamic signals, also referred to as the undirected and directed interaction, respectively (Bowyer, 2016). Connectivity appears to be central to understanding the systematic information processing organization of the brain for cognitive, sensory as well as other processes (Chen et al., 2019; Chung et al., 2012; Harrison et al., 2003; Kelso et al., 2013; Tognoli & Kelso, 2009). It offers a fundamental insight into the functional network organization of the brain (Hipp et al., 2012). However, the exact model of the synchronization among the brain regions and its functional role in cognitive, sensory, and motor tasks is still unclear (Marinazzo et al., 2011). For this reason, various kinds of model-free synchronization metrics have been proposed to measure the synchronization between the brain regions and tested on synthetic and real multichannel electrophysiological datasets to evaluate the effectiveness of these methods (Bakhshayesh et al., 2019a, 2019b; Duckrow & Albano, 2003; Greenblatt et al., 2012; He et al., 2019; He & Yang, 2021; Olcay & Karaçalı, 2019; Pereda et al., 2005; Sakkalis, 2011). These synchronization metrics were also exploited in BCI studies that proposed to use the statistical interactions between distinct regions of the brain as features (Brunner et al., 2006; Daly et al., 2012; Gu et al., 2020; Hamedi et al., 2016; Wei et al., 2007), and in biophysical studies to identify various brain disorders such as schizophrenia (Calhoun et al., 2008), autism spectrum disorder (Sarmukadam et al., 2020), depression (Peng et al., 2019), sleep-related disorders (Melia et al., 2015, 2014), mild cognitive impairment (Gómez et al., 2009), loss of vision (Bola et al., 2015) or Parkinson (Skidmore et al., 2011).

In the literature, the majority of the synchronization (i.e. connectivity)-based brain activity characterization studies disregard the dynamically changing characteristics of the brain and assume that the inter-regional synchronization profile between brain regions remains constant throughout the cognitive task periods (Brunner et al., 2006; Gonuguntla et al., 2016; Makarov et al., 2018; Olejarczyk et al., 2017; Tirsch et al., 2004; Wang et al., 2006). However, the dynamically changing and nonlinear characteristics introduce an additional challenge in elucidating the resting state as well as task-based cognitive dynamics (Hutchison et al., 2013; Ince et al., 2009; Rabinovich & Muezzinoglu, 2010; Stam, 2005; Stam et al., 2003; Zink et al., 2020). The intermittent characteristics of the inter-regional EEG/MEG synchronizations were demonstrated to be the results of transient activations/synchronizations of localized neuronal ensembles (Stam et al., 2003).

Few studies exist in the literature that try to extract and interpret the intermittent dynamical characteristics of the brain activity for modeling cognitive tasks/states. Lu et al. analyzed short-lived functional interactions of EEG channels via time–frequency cross mutual information analysis. They observed the dynamical changes of the channel synchronizations according to the task demands (Lu et al., 2011). Baker et al. used a Hidden Markov Model (HMM) to capture consistent short-lived brain states that emerge with transiently coherent spatial networks to characterize the behavior of the brain during idling conditions (Baker et al., 2014). Rodu et al. proposed a dynamical kernel canonical correlation analysis-based approach to determine the short-lasting delayed correlation patterns among electrophysiological signals (Rodu et al., 2018). Santamaria et al. identified the short-lived phase synchronized states during motor imagery tasks and used them for activity recognition purposes (Santamaria & James, 2019). Pfurtscheller et al. highlighted the emergence of short-lived somatotopically-specific brain states during motor imagery activities (Pfurtscheller et al., 2008). Gu et al. used time–frequency decomposition for EEG signals collected during lower extremity motor imagery tasks and observed short-lived frequency-specific ERD/ERS patterns (Gu et al., 2020). Ambrosi et al. proposed a particle filtering-based method to analyze the temporal variations of brain synchronization (Ambrosi et al., 2019). Hansen et al. addressed the transient nature of the synchronization between brain regions during the rest state (Hansen et al., 2015). Ren et al. analyzed the fluctuations of information integration/segregation via dynamic graph metrics and showed that during cognitive tasks a dynamic small world architecture emerges in the brain (Ren et al., 2017). Karamzadeh et al. used a dynamic time warping-based approach to track and analyze the characteristics of time-varying brain synchronization due to auditory and visual stimulus presentation (Karamzadeh et al., 2013). Li et al. proposed a conditional Granger causality analysis to track the dynamic connectivity between brain regions (Li, Lei et al., 2019). Spiegler et al. analyzed the frequency-specific time-varying phase coupling characteristics of tongue-movement imagery activity on the time–frequency domain (Spiegler et al., 2004). Dimitriadis et al. proposed a scheme that discretizes the captured short-lived phase-synchronized microstate patterns to analyze the transitory behavior of brain regions during task periods (Dimitriadis et al., 2013). Schack et al. captured the activity-specific short-lived cortical connectivity profiles during abstract and concrete noun processing (Schack et al., 2003).

All these studies stress the importance of considering the dynamic nature of the brain in characterizing electrical activity during any kind of cognitive state (Pfurtscheller et al., 2008; Vidaurre et al., 2018; Zalesky et al., 2014). Additional studies point to another related phenomenon; the emergence of systematic timing organization of synchronization of the electrical activity between different regions of the brain during cognitive tasks (Adhikari et al., 2010; Boeijinga & Lopes da Silva, 1989; Dawson, 2004; Jeong et al., 2001; Ktonas & Mallart, 1991; Na et al., 2002; Olcay & Karaçalı, 2019; Roelfsema et al., 1997). The studies that consider the systematic timing organization of brain synchronization is based on the premise that the brain coordinates the information routing between cortical regions by re-organizing the synchronization timings between the associated brain regions for each cognitive task according to the task demands (Alais et al., 1998; Dawson, 2004; Jin et al., 2012; Lin et al., 2020). In this manner, the brain integrates the localized neural activities by creating a short-lived communication window between brain regions by reciprocally modulating the synchronization of the neural activities at activity-specific timings during the information routing (Palmigiano et al., 2017). This argument was also exploited in recent studies to understand the inherent mechanism of the synchronization between brain regions which shows a dynamically changing behavior at each time point (Ren et al., 2017). These instantaneous alterations of inter-regional brain synchronization are thought to be due to the metastable characteristics (formation and dissolution of metastable states) of the brain (Kelso et al., 2013; Santamaria & James, 2019; Tognoli & Kelso, 2009; Varela et al., 2001). At the metastable regimes, brain regions dynamically summon and release each other which can be observed in terms of continuous alterations of inter-regional synchronizations. During cognitive tasks, specialized brain regions

share similar intrinsic properties and reveal strong synchronizations for short periods of time. The emergence of short-lived maximal synchronizations between brain regions can be described by communication-through-coherence (CTC) hypothesis through which segregated information over distant brain regions is integrated (Fries, 2005). As Bastos, Hari, and Mitra et al. pointed out, inter-regional synchronizations emerge with inter-regional time delays (Bastos et al., 2015; Hari & Parkkonen, 2015; Mitra et al., 2015). In our previous study, we showed that the inter-regional maximal brain synchronizations emerged at specific inter-channel time lags (Olcay & Karaçalı, 2019). In that study, however, we had only used the time lag parameter (τ) for synchronization analysis. On the other hand, according to the temporal information processing mechanism, maximal synchronization between brain regions cannot be expected to be maintained all the way from task onset to the period end since the brain is known to exhibit a dynamically changing characteristics. In order to address this limitation, in this study, we introduced two new timing parameters (Δt, w) to accurately find when the characteristic synchronization emerges and vanishes between channel pairs.

Supporting this hypothesis, Kirschner et al. identified the task-specific brain synchronization patterns that emerged consistently during a cognitive task and determined that these synchronization patterns remain more active than some of the inter-regional synchronizations observed within the default mode network (Kirschner et al., 2012). In a face recognition study, Wang et al. determined that the phase coherence simultaneously increases at infra-slow frequency bands between task-specific brain regions. They also suggested that the synchronization lag among the oscillatory activities becomes smaller for faster and more accurate inter-regional communication and that the inter-regional synchronization lag reorganizes to adapt to the requirements of cognitive activities (Wang et al., 2019). Hermanto et al. stated that the brain should generate similar synchronization patterns at similar timings among its regions for each trial of a particular cognitive task to meet the task-specific demands (Hermanto et al., 2013). These findings suggest that an accurate characterization of cognitive tasks can be achieved by capturing and using activity-specific timings at which the systematic and characteristic inter-regional short-lived synchronization occurs (Bassett et al., 2006; Jin et al., 2012).

The principal goal of the present study is to determine the timings of the activity-specific short-lived synchronizations between the EEG channels for different cognitive tasks. To that end, we propose a method that determines the activity-specific short-lived inter-channel synchronization timings that elicited the most significant maximal average pairwise synchronization calculated across all task periods separately for each motor imagery activity and each channel pair. The short-lasting maximal synchrony between the brain electrical signals during a cognitive task can be thought of as evidencing cognitive task-specific information exchange/flow between the corresponding brain regions and possibly also in specific frequency bands (Gonuguntla et al., 2016; Maars & Lopes Da Silva, 1983; Wibral et al., 2011; Zanon et al., 2018), which may further signify the presence of an activity-specific functional integration mechanism (Jin et al., 2006; Rubinov & Sporns, 2010; Tognoli & Kelso, 2009). The three timing parameters we use to calculate pairwise channel synchrony are: Δt for latency of maximally synchronized signal segments from activity onset ($t = 0$), τ for the time lag between maximally synchronized signal segments, and w for the length of the maximally synchronized signal segments (please see Fig. 1). In order to determine the values of these timing parameters, we used a sliding short-duration time window as done in Hutchison et al. (2013) and Xu et al. (2008) for each task period and channel pair to track the dynamically evolving synchronization patterns for varying time lag (τ) and latency (Δt) values. Then, we averaged the synchronizations obtained from corresponding task periods and channel pairs to obtain a common synchronization behavior. Finally, we used a heuristic search method to determine the associated timing parameter triplets that elicit maximal average synchronization.

As the synchronization measures, we used cosine-based similarity (Olcay & Karaçalı, 2019; Sargolzaei et al., 2015), wavelet bi-coherence (Bandrivskyy et al., 2004; Makarov et al., 2018), phase-locking value (PLV) (Lachaux et al., 1999; Varela et al., 2001), phase coherence value (PCV) (Bakhshayesh et al., 2019b; Tass et al., 1998), linearized mutual information (LMI) (Jin et al., 2010), and cross-correntropy (Liu et al., 2007; Santamaría et al., 2006). As each synchronization method is based on different mathematical assumptions and utilizes different features of the electrophysiological signals to evaluate the synchronization, their performances elucidated the mechanism of brain synchronization for motor imagery (Wang et al., 2014).

The activity-specific timing parameter triplets for each channel pair and each type of motor imagery activity were then used in a motor imagery activity recognition framework whereby we used the activity-specific timing parameter triplets to calculate the inter-channel short-lived synchronizations and used them as features in a task recognition setting. The resulting recognition performances indicate that the proposed framework captures the timings of short-lived and activity-specific inter-channel synchronizations. With potentially descriptive information related to the corresponding cognitive activity, these results also suggest that this approach can be used in a cognitive activity recognition framework.

The remainder of this paper is organized as follows: In Section 2, we describe the datasets along with the proposed method, as well as the synchronization measures used in this study. In Section 3, we present the recognition performance results that compare channel synchronization values obtained for different tasks calculated using the activity-specific timing parameter triplets. In Section 4, we discuss the results. The final section concludes the paper.

2. Materials and methods

In this section, we describe the methodology that pertains to the study, along with a description of the EEG datasets. Mathematical details are also provided including the definition of the synchronization measures as well as the optimization procedure to identify activity-specific timing parameters for each channel pair.

2.1. Datasets

In this study, we used two publicly available motor imagery datasets, BCI Competition-III dataset IVa (Blankertz et al., 2006; Dornhege et al., 2004) and PhysioNet Motor Movement/Imagery dataset (Goldberger et al., 2000; Schalk et al., 2004). The former dataset was collected using 118 electrodes according to the extended international 10/20 system. The original sampling frequency of the recording system was 1 kHz. This study was carried out using a downsampled version of this dataset to 100 Hz which is also available for download at the competition website. This dataset was collected from 5 subjects performing right hand/right foot motor imagery activity with 140 task periods each. Every motor imagery activity period lasted 3.5 s.

The latter dataset was collected via BCI2000 using international 10/10 system with 64 channels at a sampling frequency of 160 Hz. It includes recordings from 109 subjects performing

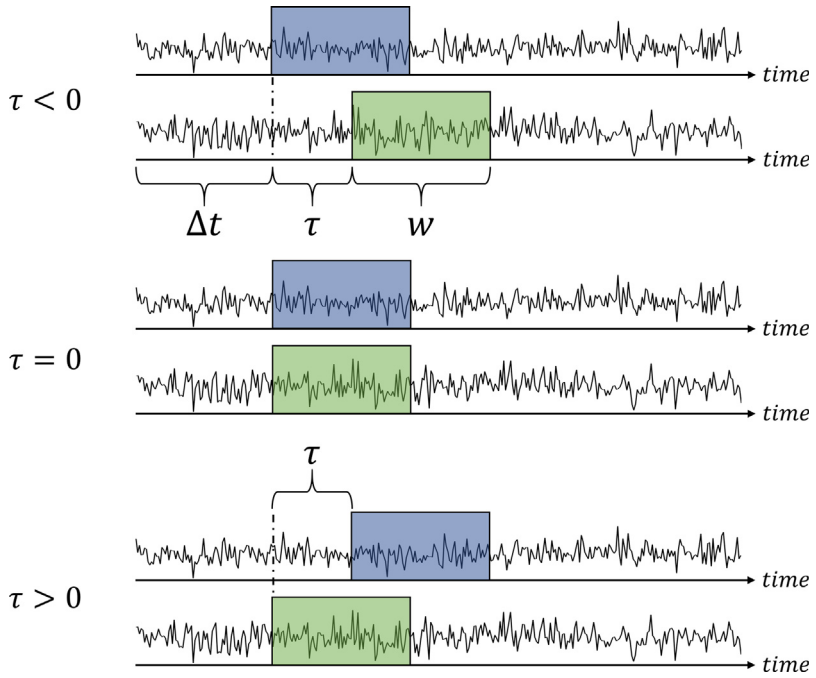

Fig. 1. The illustration of the timing parameters Δt, τ, and w used to determine pairwise short-lived synchronization between two EEG channels. Δt stands for latency of characteristic synchronization from activity onset, τ for time lag between synchronized the signal segments, and w for duration of the characteristic synchronization. We demonstrated the three cases in which time-directional synchronization calculated for $\tau < 0$, $\tau = 0$, and $\tau > 0$.

Table 1
The progression of the EEG recording sessions for PhysioNet dataset.

Task name	Motor execution sessions	Motor imagery sessions
Right/Left fist	3, 7, 11	4, 8, 12
Both fists/Both feet	5, 9, 13	6, 10, 14

right/left fist and both feet/both fists motor movement/imagery tasks. Each subject repeated movement/imagery task periods in three sessions. Each task period lasted 4.1 s. Prior to the motor movement/imagery sessions, there exist two 1-minute eyes open/close recording sessions. The progression of the motor execution/imagery sessions is given in Table 1. Each motor movement/imagery session contains 15 task and 15 rest periods.

In total, we used all 280 motor imagery activity periods collected from each subject of the BCI Competition-III dataset, and of the PhysioNet dataset, we used all 45 motor imagery activity periods of all three right/left fist motor imagery sessions of the first 20 subjects for training and testing purposes of the proposed method. For both datasets, prior to the analysis, we re-referenced the signals to the common average to minimize the effects of volume conduction and referencing problems (Lotte, 2008; Ludwig et al., 2009; McFarland et al., 1997). We then filtered the EEG signals with a finite-impulse-response (FIR) filter with a pass band frequency range of 8–30 Hz to obtain the motor imagery related brain dynamics (Höller et al., 2013; Pfurtscheller et al., 2000; Wei et al., 2007; Yuan & He, 2014). The choice of a FIR filter was made to avoid phase distortions of infinite-impulse-response filters (Jian et al., 2017). As the final step of pre-processing, we extracted the signals of the motor imagery task periods using the timing annotations along with the corresponding labels indicating the associated motor imagery task for the subsequent analysis.

2.2. Synchronization measures

In order to capture the timings of the activity-specific short-lived synchronization between the EEG channels, we used six different synchronization measures listed below.

- Cosine-based similarity (Herff et al., 2019; Olcay & Karaçalı, 2019; Sargolzaei et al., 2015)
- Wavelet bi-coherence (Makarov et al., 2018)
- Phase Locking Value (Lachaux et al., 1999; Varela et al., 2001)
- Phase Coherence Value (Bakhshayesh et al., 2019b; Tass et al., 1998; Ziqiang & Puthusserypady, 2007)
- Linearized Mutual Information (Jin et al., 2010)
- Cross-Correntropy (Liu et al., 2007; Principe, 2010; Santamaría et al., 2006).

We used Vasicek's bias-corrected entropy estimation method (Ibrahim Al-Omari, 2014; Vasicek, 1976) to calculate the entropies of the phase differences for the phase coherence value method. Furthermore, we used complex Morlet wavelets to calculate the wavelet transforms of the EEG signals for the wavelet bi-coherence method. Finally, we adopted a Laplacian kernel for the cross-correntropy method (Rao et al., 2011).

Prior to the synchronization calculation, we extracted the signal segments of each task period from each channel represented by $s_{i,n}^{\Delta t,w} = s_i\left(t'\right)|_{t'\in[t_n+\Delta t,t_n+\Delta t+w]}$ where the signal segment extracted from task period n and channel i starts at Δt milliseconds from the activity onset t_n and lasts for w milliseconds. Similarly, $s_{j,n}^{\Delta t+\tau,w} = s_j\left(t'\right)|_{t'\in[t_n+\Delta t+\tau,t_n+\Delta t+\tau+w]}$ represents the signal segment extracted from task period n and channel j that starts at $\Delta t+\tau$ milliseconds from the activity onset t_n and lasts for w milliseconds (please see Figs. 1 and 2). Thus, Δt represents the latency of maximally synchronized signal segments from activity onset, τ represents the time lag between two maximally synchronized signal segments, and w represents the length (i.e., duration) of the maximally synchronized signal segments. Note that while τ can take positive or negative values, Δt takes values that are greater than or equal to zero only. Consequently, $s_{j,n}^{\Delta t+\tau,w}$ may lead or lag $s_{i,n}^{\Delta t,w}$ on the time axis.

2.3. Determination of activity-specific timing parameter triplets

In this study, the main target is to capture the optimal timing parameter triplets for each specific cognitive activity and channel

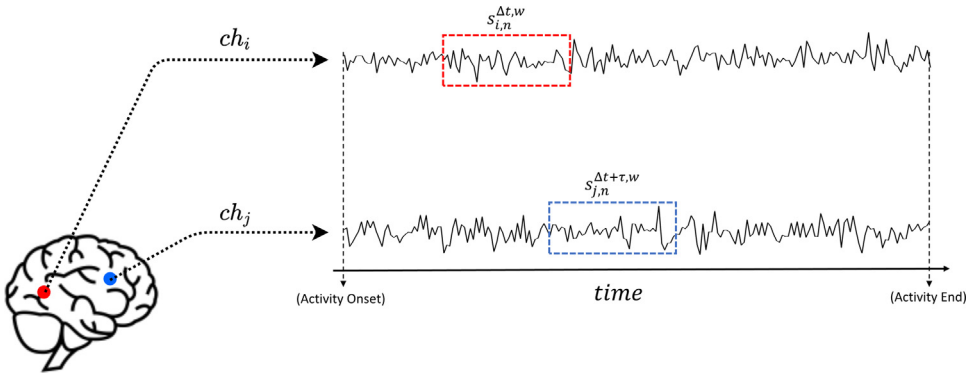

Fig. 2. Illustration of short-lived signal segments $s_{i,n}^{\Delta t,w}$ and $s_{j,n}^{\Delta t+\tau,w}$ obtained from EEG channels i and j for task period n. Note that here, τ takes a positive value, indicating that the ith channel is leading the jth channel.

pair that elicit the maximal synchronization of the channels. In that context, we adopted the heuristic search strategy described below as the EEG signals and their short-lived synchronization estimates are quite noisy. In such cases, using well-known search methods such as gradient descent and the Nelder–Mead are prone to get stuck in the 3-dimensional timing parameter space.

In order to determine the activity-specific timing parameter triplets $\{\Delta t, \tau, w\}$ for each channel pair and each type of cognitive activity, we adopted a sliding time window based search method with a fixed length of 300 ms as in Bola et al. (2015) and Roelfsema et al. (1997). In this procedure, we first calculated the short-lived synchronization between the signal segments obtained for each channel pair (i, j) and training task period n for varying $\Delta t \in [0 \text{ ms}, 2000 \text{ ms}]$ (Chung et al., 2012; Neuper et al., 2009) and $\tau \in [-125 \text{ ms}, 125 \text{ ms}]$ (Olcay & Karaçalı, 2019) at a fixed duration of $w = 300$ ms as

$$D_{i,j}(\Delta t, \tau, n) = S\left(s_{i,n}^{\Delta t,300 \text{ ms}}, s_{j,n}^{\Delta t+\tau,300 \text{ ms}}\right) \tag{1}$$

where $S(\cdot,\cdot)$ denotes the synchronization measure of choice. We then calculated the average synchronization across the training task periods of the same cognitive activity type for each channel pair (i, j) as

$$\overline{D}_{i,j}^{A_{1/2}}(\Delta t, \tau) = \frac{1}{|I_{1/2}|} \sum_{n \in I_{1/2}} D_{i,j}(\Delta t, \tau, n) \tag{2}$$

where $\overline{D}_{i,j}^{A_{1/2}}(\Delta t, \tau)$ is the average synchronization matrix calculated across the corresponding training task periods, and I_1 and I_2 are the indices of the training task periods belonging to activity types A_1 and A_2, respectively. Since the aim of this study is to analyze the short-lived brain interactions, we adopted a quantile (or alternatively percentile) based thresholding to capture the important synchronization dynamics as used in Zink et al. (2020). Next, we thresholded the average synchronization values $\overline{D}_{i,j}^{A_{1/2}}(\Delta t, \tau)$ with respect to the 99% quantiles of cumulative distribution function (CDF) obtained from all values $\left\{\overline{D}_{i,j}^{A_{1/2}}(\Delta t, \tau)\right\}$ for all combinations of Δt and τ. This revealed candidate short-lived synchronization patterns that extend along the Δt axis, that were then subjected to statistical evaluation.

For the statistical evaluation, we identified the timing parameter triplets that correspond to each of candidate short-lived synchronization patterns. Note that a synchronization pattern observed at $\tau = \tau_0$ and $\Delta t_1 \leq \Delta t \leq \Delta t_2$ suggests significant synchronization between $s_{i,n}^{\Delta t_1, \Delta t_2 - \Delta t_1 + 300 \text{ ms}}$ and $s_{j,n}^{\Delta t_1+\tau_0, \Delta t_2 - \Delta t_1 + 300 \text{ ms}}$ (please see Fig. 3). The statistical test evaluated the average synchronizations observed for each such triple timing parameter against zero for each channel pair (i, j) in case multiple candidate patterns emerged and selected the one with the lowest P-value observed as a result of t-test. Consequently, we identified the optimal timing parameter triplet that maximizes the statistical significance of channel synchronizations for each activity type and for each channel pair separately.

2.4. Proposed framework

In this section we provide the details of the proposed framework summarized by the flow diagram in Fig. 4.

In the training phase, we determined the activity-specific timing parameter triplets $\left\{\Delta t_{i,j}^{A_1}, \tau_{i,j}^{A_1}, w_{i,j}^{A_1}\right\}$ and $\left\{\Delta t_{i,j}^{A_2}, \tau_{i,j}^{A_2}, w_{i,j}^{A_2}\right\}$ for cognitive activities A_1 and A_2 for each channel pair (i, j). Next, we used the activity-specific timing parameter triplets to calculate inter-channel synchronization values of all channel pairs and then collected these synchronization values into a feature vector for each training task period. Thus, the training feature vector ξ_ℓ for the training task period indexed by ℓ is constructed as

$$\xi_\ell = \begin{bmatrix} S\left(s_{1,\ell}^{\Delta t_{1,2}^{A_1}, w_{1,2}^{A_1}}, s_{2,\ell}^{\Delta t_{1,2}^{A_1}+\tau_{1,2}^{A_1}, w_{1,2}^{A_1}}\right) \\ S\left(s_{1,\ell}^{\Delta t_{1,3}^{A_1}, w_{1,3}^{A_1}}, s_{3,\ell}^{\Delta t_{1,3}^{A_1}+\tau_{1,3}^{A_1}, w_{1,3}^{A_1}}\right) \\ \vdots \\ S\left(s_{M-2,\ell}^{\Delta t_{M-2,M}^{A_1}, w_{M-2,M}^{A_1}}, s_{M,\ell}^{\Delta t_{M-2,M}^{A_1}+\tau_{M-2,M}^{A_1}, w_{M-2,M}^{A_1}}\right) \\ S\left(s_{M-1,\ell}^{\Delta t_{M-1,M}^{A_1}, w_{M-1,M}^{A_1}}, s_{M,\ell}^{\Delta t_{M-1,M}^{A_1}+\tau_{M-1,M}^{A_1}, w_{M-1,M}^{A_1}}\right) \\ S\left(s_{1,\ell}^{\Delta t_{1,2}^{A_2}, w_{1,2}^{A_2}}, s_{2,\ell}^{\Delta t_{1,2}^{A_2}+\tau_{1,2}^{A_2}, w_{1,2}^{A_2}}\right) \\ S\left(s_{1,\ell}^{\Delta t_{1,3}^{A_2}, w_{1,3}^{A_2}}, s_{3,\ell}^{\Delta t_{1,3}^{A_2}+\tau_{1,3}^{A_2}, w_{1,3}^{A_2}}\right) \\ \vdots \\ S\left(s_{M-2,\ell}^{\Delta t_{M-2,M}^{A_2}, w_{M-2,M}^{A_2}}, s_{M,\ell}^{\Delta t_{M-2,M}^{A_2}+\tau_{M-2,M}^{A_2}, w_{M-2,M}^{A_2}}\right) \\ S\left(s_{M-1,\ell}^{\Delta t_{M-1,M}^{A_2}, w_{M-1,M}^{A_2}}, s_{M,\ell}^{\Delta t_{M-1,M}^{A_2}+\tau_{M-1,M}^{A_2}, w_{M-1,M}^{A_2}}\right) \end{bmatrix} \tag{3}$$

where M denotes the total number of channels (i.e., $M = 118$ for BCI Competition-III dataset, $M = 64$ for PhysioNet dataset). After constructing the training feature vectors, we performed a feature selection procedure to determine the most discriminative features. To that end, we calculated the Fisher's ratio of each

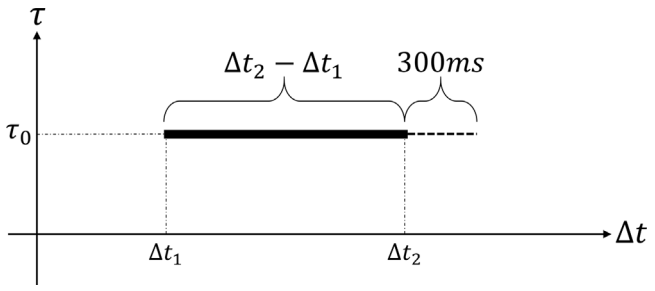

Fig. 3. An illustration of the heuristic optimization scheme to determine the timing parameter triplet characterizing the maximal synchronization for a channel pair (i, j). After thresholding, the optimal timing parameter triplet for this case is determined as $(\Delta t, \tau, w) = (\Delta t_1, \tau_0, \Delta t_2 - \Delta t_1 + 300 \text{ ms})$.

feature using (Duda & Hart, 2000)

$$F_\alpha = \frac{\left|\mu_{\alpha,A_1} - \mu_{\alpha,A_2}\right|}{\sigma_{\alpha,A_1} + \sigma_{\alpha,A_2}} \tag{4}$$

where μ_{α,A_1} and μ_{α,A_2} are the mean and σ_{α,A_1} and σ_{α,A_2} are the standard deviation values of the feature indexed by α across the training feature vectors of activities A_1 and A_2, respectively. We selected the features which elicited a Fisher's ratio higher than the mean plus two times standard deviation of all Fisher's ratios. Finally, we trained classifiers on the reduced training feature vectors. In this study, we used three different classification methods, namely Fisher's linear discriminant (FLD), linear support vector machines (linear SVM), and nonlinear (radial basis function) support vector machines (nonlinear SVM). The kernel width parameter γ for the radial basis function of nonlinear SVM was calculated according to

$$\gamma = \sqrt{\frac{1}{L\,(L-1)} \sum_{i=1}^{L-1} \sum_{j=i+1}^{L} \left\| \xi_i - \xi_j \right\|^2} \tag{5}$$

where L denotes the total number of training feature vectors.

In the test phase, we constructed the test feature vectors ξ for each test task periods using the activity-specific timing parameter triplets obtained in the training phase as

$$\xi = \begin{bmatrix} S\left(s_1^{\Delta t_{1,2}^{A_1}, w_{1,2}^{A_1}}, s_2^{\Delta t_{1,2}^{A_1}+\tau_{1,2}^{A_1}, w_{1,2}^{A_1}}\right) \\ S\left(s_1^{\Delta t_{1,3}^{A_1}, w_{1,3}^{A_1}}, s_3^{\Delta t_{1,3}^{A_1}+\tau_{1,3}^{A_1}, w_{1,3}^{A_1}}\right) \\ \vdots \\ S\left(s_{M-2}^{\Delta t_{M-2,M}^{A_1}, w_{M-2,M}^{A_1}}, s_M^{\Delta t_{M-2,M}^{A_1}+\tau_{M-2,M}^{A_1}, w_{M-2,M}^{A_1}}\right) \\ S\left(s_{M-1}^{\Delta t_{M-1,M}^{A_1}, w_{M-1,M}^{A_1}}, s_M^{\Delta t_{M-1,M}^{A_1}+\tau_{M-1,M}^{A_1}, w_{M-1,M}^{A_1}}\right) \\ S\left(s_1^{\Delta t_{1,2}^{A_2}, w_{1,2}^{A_2}}, s_2^{\Delta t_{1,2}^{A_2}+\tau_{1,2}^{A_2}, w_{1,2}^{A_2}}\right) \\ S\left(s_1^{\Delta t_{1,3}^{A_2}, w_{1,3}^{A_2}}, s_3^{\Delta t_{1,3}^{A_2}+\tau_{1,3}^{A_2}, w_{1,3}^{A_2}}\right) \\ \vdots \\ S\left(s_{M-2}^{\Delta t_{M-2,M}^{A_2}, w_{M-2,M}^{A_2}}, s_M^{\Delta t_{M-2,M}^{A_2}+\tau_{M-2,M}^{A_2}, w_{M-2,M}^{A_2}}\right) \\ S\left(s_{M-1}^{\Delta t_{M-1,M}^{A_2}, w_{M-1,M}^{A_2}}, s_M^{\Delta t_{M-1,M}^{A_2}+\tau_{M-1,M}^{A_2}, w_{M-1,M}^{A_2}}\right) \end{bmatrix} \tag{6}$$

After the constructing the test feature vectors, we extracted the features that were identified in the training phase, applied the classifiers constructed earlier on the reduced test feature vectors and correspondingly assigned the associated task period either to A_1 or A_2.

To be clearer, we constructed the algorithmic steps in tabular form for finding activity-specific timing parameter triplets, and the classification framework that we adopted in this study (please see Tables 2 and 3).

2.5. Comparative analysis

We employed conventional CSP and AR modeling methods to compare the performance of the proposed method. We calculated the CSP filters on the training task periods by setting the number of eigenvectors $m = 3$ in accordance with the literature and filtered all training and test task periods by CSP filters (Blankertz

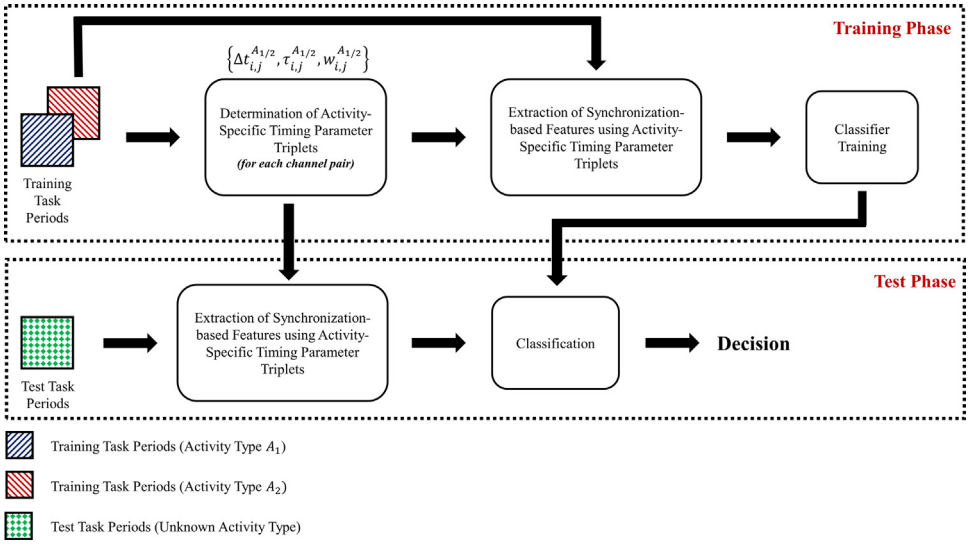

Fig. 4. Illustration of the operational flow diagram of the proposed short-lived synchronization based cognitive activity characterization framework.

Table 2
The algorithmic steps of finding activity-specific timing parameters triplets from the training set.

Algorithm-1:	Finding activity-specific timing parameter triplets
Step-1	For the channel pair (i, j), calculate inter-channel synchronizations for $\Delta t \in [0 \text{ ms } 2000 \text{ ms}]$, $\tau \in [-125 \text{ ms } 125 \text{ ms}]$ via $w = 300$ ms length sliding time window for each training task period of activity A.
Step-2	Calculate the average the synchronization values across training task periods of activity A.
Step-3	Set the threshold to %99 quantile of average synchronization values. Then, compare each entry of average synchronization matrix with the threshold.
Step-4	Determine the timings of each of synchronization patterns remaining after thresholding. Use each one of these candidate timings to extract the signal segments from corresponding training task periods.
Step-5	Calculate the synchronization between the extracted signal segments. Apply t-test to these synchronization values to determine P-value of each timing parameter.
Step-6	Identify the timing parameter triplet for channel pair (i, j) and activity A, which elicited the smallest P-value as activity-specific timing parameter triplet (i.e., $\left\{\Delta t_{i,j}^{A}, \tau_{i,j}^{A}, w_{i,j}^{A}\right\}$). Repeat these calculations from the steps 1–6 for all channel pairs.

Table 3
The algorithmic steps of the classification framework.

Algorithm-2:	The classification framework
Step-1	Use 8–30 Hz bandpass filter and CAR to filter the data spectrally and spatially.
Step-2	Use **Algorithm-1** to obtain the A_1 activity-specific timing parameter triplets for each channel pair.
Step-3	Use **Algorithm-1** to obtain the A_2 activity-specific timing parameter triplets for each channel pair.
Step-4	Use both A_1 and A_2 activity-specific timing parameter triplets to construct training feature vectors.
Step-5	Calculate the Fisher ratio of each feature. Identify the features that elicited higher than mean plus two standard deviation of Fisher ratios of all features.
Step-6	Train the classifiers by using reduced training feature vectors.
Step-7	Use both A_1 and A_2 activity-specific timing parameter triplets to construct reduced test feature vectors.
Step-8	Determine the category of each test feature by using the classifier trained in step-6

et al., 2008). Then, we extracted the log-variance features from CSP-filtered task periods. For AR modeling, we used a least-squares method to calculate the univariate model coefficients over signal segments of one-second sliding time windows with %50 percent overlap and concatenated them together to incorporate the dynamic changes of the spectral information of the electrophysiological activity as adopted in the past literature (Golub & Saunders, 1970; Gürkan et al., 2014; Ince et al., 2007; Kuruoğlu, 2002). We set the AR model order of each channel to six as in Anderson et al. (1998) and Ince et al. (2007) unlike in McFarland and Wolpaw (2008) due to the limited number of signal samples in the sliding time window. Next, we performed a feature ranking via the Fisher's ratio to select the most discriminative AR coefficients for activity recognition. We selected the AR features that exceeded mean plus two times standard deviation calculated using all Fisher ratios of all AR features. We then trained the classifiers using the reduced training AR features. Similarly, we extracted the features from each test task period using the same procedure adopted for training AR based features. We finally obtained the reduced test feature vectors for performance comparison.

3. Results

We used two distinct chronological cross-validation scenarios (i.e. scenario-1 and scenario-2) to evaluate the performance of our brain activity characterization method for different training set sizes as in our previous study (Olcay & Karaçalı, 2019). The details of the chronological partitioning of the datasets for two different training/testing scenarios are shown in Table 4.

We determined the activity-specific timing parameter triplets for each type of motor imagery activity using the training task periods for each subject individually in both BCI Competition-III dataset IVa (i.e., right hand/right foot imagery movement) and PhysioNet dataset (right/left fist imagery movement). Afterwards, we constructed the synchronization-based feature vectors as in Eq. (3) and (6) and carried out training and testing procedures described earlier. Average classification performances are shown in Figs. 5–8, where in Figs. 5 and 6, we presented the average performances obtained using the six different synchronization measures obtained via three different classifiers. In Figs. 7 and 8, we presented the maximum performances obtained via the currently proposed method, the earlier τ-based method developed by our group (Olcay & Karaçalı, 2019), the common spatial patterns (CSP) method (Blankertz et al., 2008; Ramoser et al., 2000), and the univariate autoregressive (AR) modeling based method (Anderson et al., 1998). Note that the last two are benchmark methods in the mental imagery activity related brain activity recognition literature (Coyle et al., 2005; Pfurtscheller et al., 2000). The results show that the proposed method trails the earlier τ-based and CSP methods on the BCI Competition-III dataset IVa dataset while surpassing them significantly on the PhysioNet dataset. Interestingly, the univariate AR model-based method performed no better than random classification for the most part.

In order to provide additional insights on these results, we identified the most frequently selected channel pairs during feature selection in scenario-2 that has a larger collection of training task periods. We then carried out unpaired two-tailed t-tests among the synchronization values between contending motor imagery task periods and obtained the P-values of these synchronizations for each subject. We corrected the P-values of the channel synchronizations via Benjamini–Hochberg's (B–H) method to minimize the type-I error rates observed during statistical testing (Benjamini & Hochberg, 1995). Finally, we calculated the geometric means of the corrected P-values of the synchronization values for each channel pair across all subjects. The most significant three channel pairs and their corrected P-values obtained for BCI Competition-III dataset IVa were CCP5-CP3 ($P < 0,001$), C3-CCP3 ($P < 0,001$) and C5-CCP5 ($P < 0,001$) for right foot motor imagery, F3-CFC3 ($P < 0,001$), FFC3-FC3 ($P < 0,001$), and FC1-C3 ($P < 0,001$) for right hand motor imagery tasks. The three channel pairs that exhibit the most significant short-lived synchronization for the PhysioNet Motor Movement/Imagery dataset were FPz-FT7 ($P > 0,05$), FP2-FT7 ($P > 0,05$), and FP1-FT7 ($P > 0,05$) for left fist motor imagery, FPz-T10 ($P > 0,05$), FP2-F8 ($P > 0,05$), and FP2-T10 ($P > 0,05$) for right fist motor imagery tasks. Note, however, that the P-values obtained from the PhysioNet dataset are above the significance threshold ($P < 0,05$). A second evaluation of the PhysioNet dataset by discarding the subjects that elicited a recognition performance below 64% in scenario-2 in accordance with Athif and Ren (2019), Müller-Putz et al. (2007) and Park

Table 4
The partitioning of training and test task periods for different chronological cross validation scenarios in which training data precedes the testing data.

	Scenario-1	Scenario-2
PhysioNet	Task periods in session 4 used for training, task periods in sessions 8 and 12 used for testing	Task periods in sessions 4 and 8 used for training, task periods in sessions 12 used for testing
BCI Comp.-III	First %33 of all periods used for training; the remaining task periods used for testing	First %67 of all periods used for training; the remaining task periods used for testing

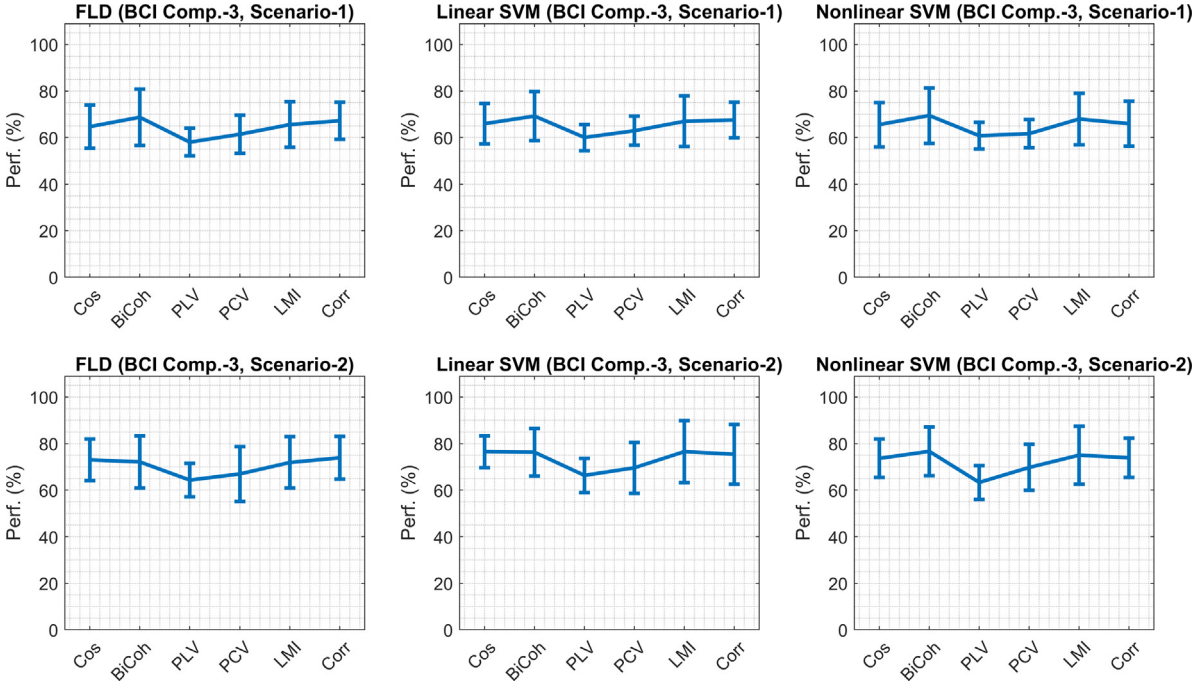

Fig. 5. Average classification performances obtained across 5 subjects for BCI Competition-III dataset IVa for both scenarios.

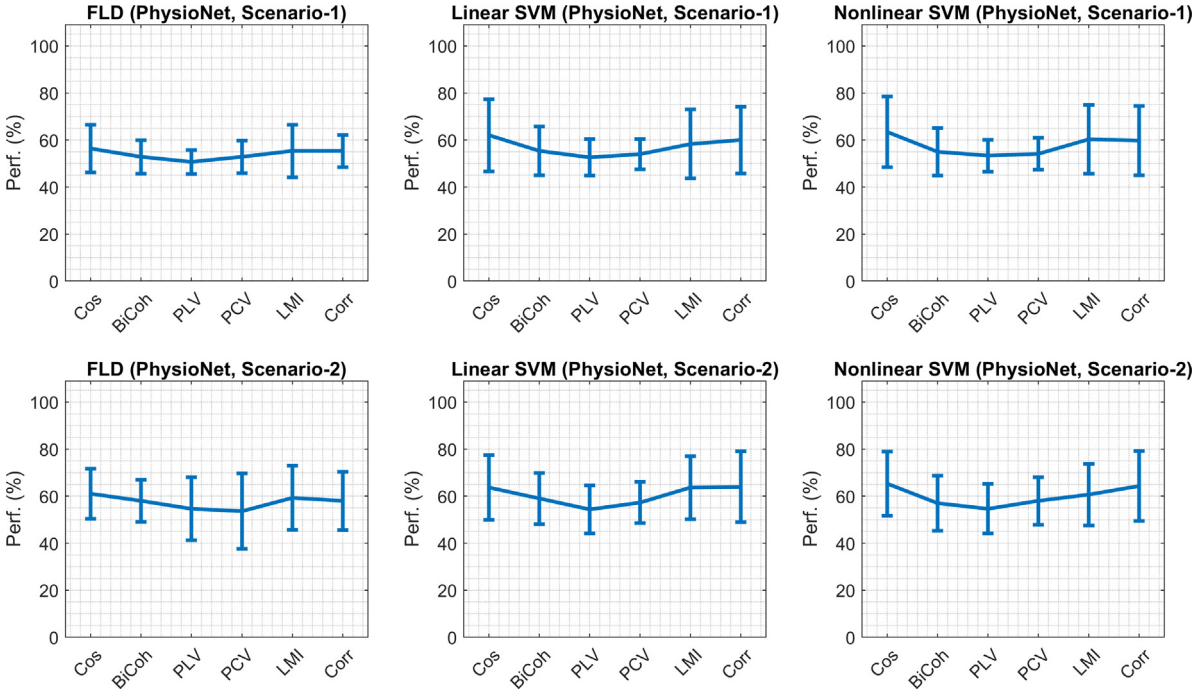

Fig. 6. Average classification performances obtained across first 20 subjects for PhysioNet Motor Movement/Imagery dataset for both scenarios.

et al. (2014) revealed channel pairs with significant task-specific synchronizations: The three channel pairs that elicited the most significant synchronizations were FPz-FT7 ($P < 0,05$), FP2-FT7 ($P < 0,05$), and FP1-FT7 ($P < 0,05$) for left fist motor imagery, FP2-F8 ($P < 0,05$), FPz-F8 ($P < 0,05$), and FPz-T10 ($P < 0,05$) for right fist motor imagery tasks.

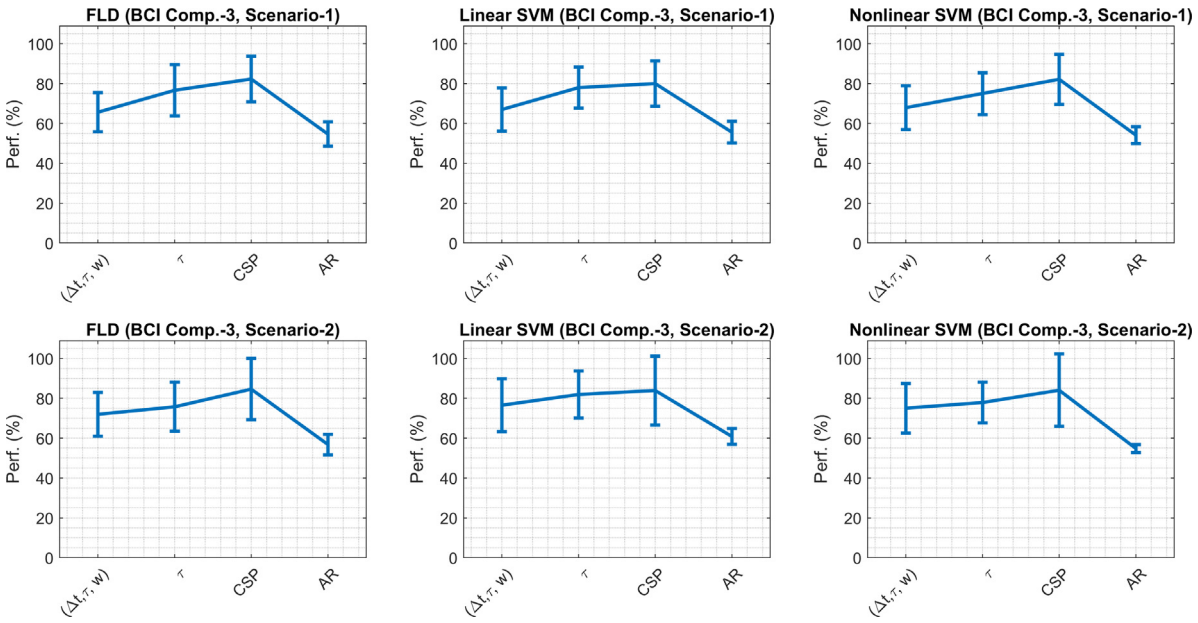

Fig. 7. Average correct classification rates of best performing configurations of maximum average performances obtained from currently proposed $\{\Delta t, \tau, w\}$ method along with τ-based, CSP, and autoregressive methods (BCI Competition-III dataset IVa). For $\{\Delta t, \tau, w\}$ method, we used linear mutual information, and we used Kraskov's mutual information estimator for the τ-based method.

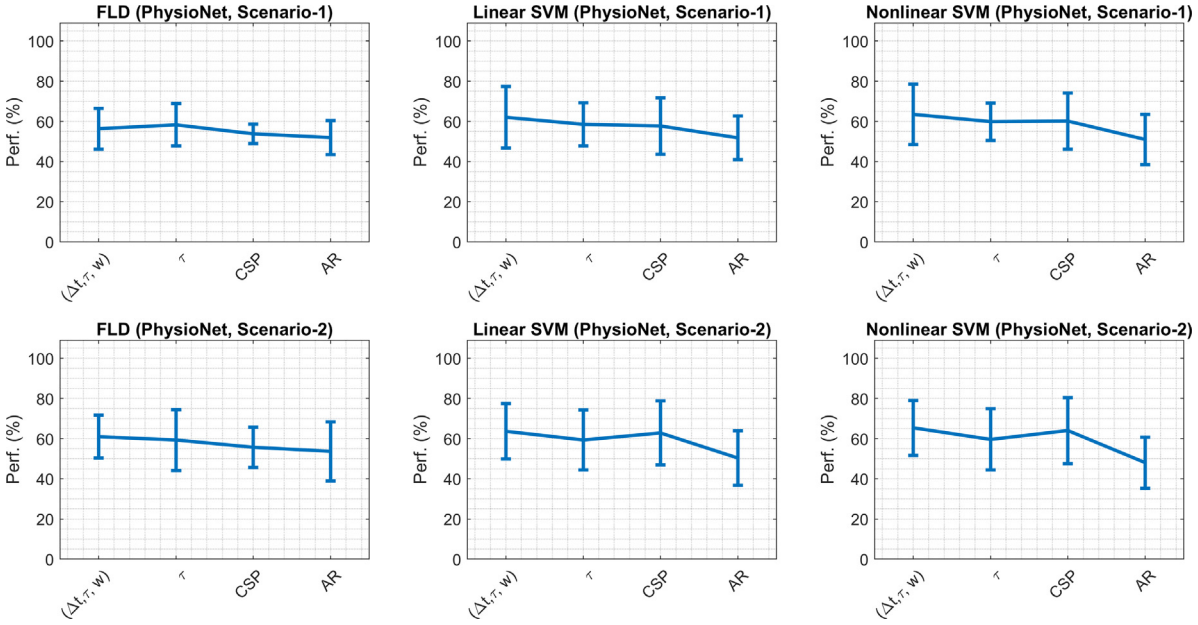

Fig. 8. Average correct classification rates of best performing configurations of maximum average performances obtained from currently proposed $\{\Delta t, \tau, w\}$ method along with τ-based, CSP, and autoregressive methods (PhysioNet dataset). For $\{\Delta t, \tau, w\}$ method, we used cosine similarity, and we used Kraskov's mutual information estimator for the τ-based method.

In order to elucidate the dynamics of task-specific channel synchronizations, we plotted the average synchronizations calculated on the CCP5-CP3 channel pair for right foot and F3-CFC3 pair for right hand motor imagery activity obtained at different $\{\Delta t, \tau\}$ combinations for the subject *al* of the BCI Competition-III dataset IVa during scenario-2 as used by the heuristic optimization scheme to determine the corresponding optimal timing parameter triplet. In Figs. 9 and 10, we presented the average synchronization values calculated using different $\{\Delta t, \tau\}$ parameters for the right foot and right hand motor imagery activities. The plots in these figures reveal that maximal synchronization is observed for this subject's CCP5-CP3 channels for $\tau = 0$ and Δt varying between 1540–1860 ms, corresponding to a timing parameter triplet of $\{\Delta t, \tau, w\} = \{1540\text{ ms}, 0\text{ ms}, 620\text{ ms}\}$. Similarly, the synchronization pattern observed for channels F3-CFC3 corresponded to the timing parameter triplet $\{\Delta t, \tau, w\} = \{580\text{ ms}, 0\text{ ms}, 1240\text{ ms}\}$.

Likewise, we plotted both average synchronization as well as the candidate synchronization patterns between channels Fp2-F8 and FPz-FT7 of the best performing PhysioNet subject (S004) for both right and left fist motor imagery activity in Figs. 11 and 12, respectively. Note that compared to the averaged synchronization patterns observed for the BCI Competition subject, these patterns are much noisier and the distinction between maximal synchronization pattern and the rest is much less clear.

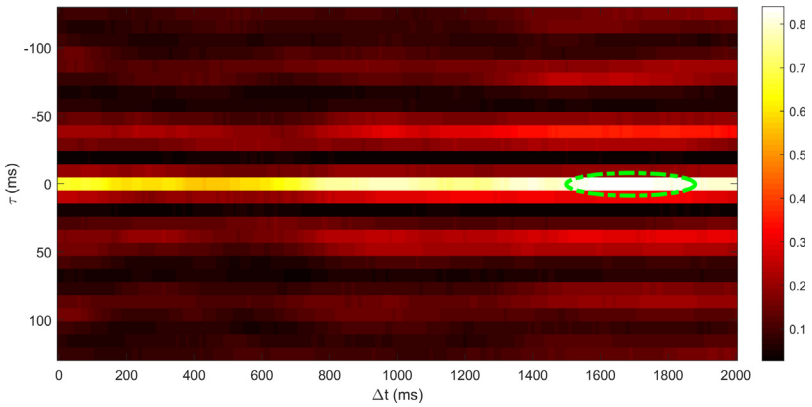

Fig. 9. The illustration of the average synchronization values between CCP5-CP3 channels calculated for each $\{\Delta t, \tau\}$ combination for right foot motor imagery activity. The green ellipse represents the candidate maximal synchronization pattern. We used linearized mutual information method to calculate the synchronization values of subject *al* who elicited the most successful recognition performance for BCI Competition-III dataset IVa.

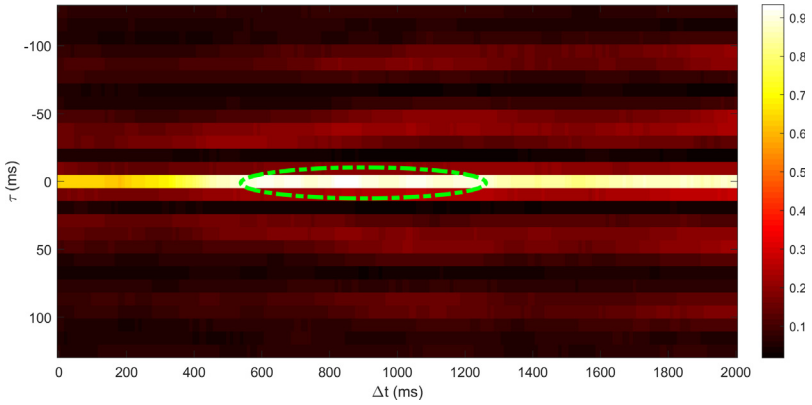

Fig. 10. The illustration of the average synchronization values between F3-CFC3 channels calculated for each $\{\Delta t, \tau\}$ combination for right hand motor imagery activity. The green ellipse represents the candidate maximal synchronization patterns. We used linearized mutual information method to calculate the synchronization values of subject *al* who elicited the most successful recognition performance for BCI Competition-III dataset IVa.

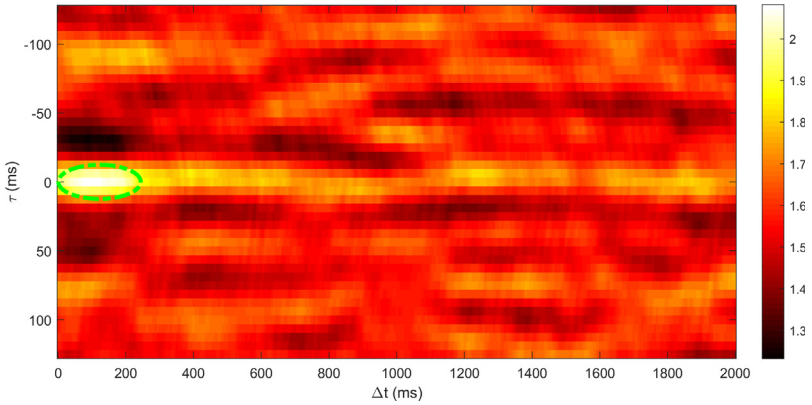

Fig. 11. The illustration of the average synchronization values between FPz-FT7 channels calculated for each $\{\Delta t, \tau\}$ combination for left fist motor imagery activity. The green ellipse represents the candidate maximal synchronization patterns. We used cosine similarity method to calculate the synchronization values of subject S004 who elicited the most successful recognition performances for the PhysioNet Motor Movement/Imagery dataset.

We presented the candidate synchronization patterns obtained for different type of motor imagery tasks in Figs. 9–12. In Tables 5 and 6, we presented the activity-specific timings for the most significant channel pairs identified for different motor imagery tasks for both BCI Competition-III dataset IVa and PhysioNet Motor Movement/Imagery dataset, respectively. Note that we presented the timings of all of the five subjects in former dataset; however, and we presented the timings of the subjects where the 64% recognition performance threshold was exceeded. It is interesting to note that the time lag values are near or equal to zero for the most significant channel pairs.

4. Discussion

Our main motivation for proposing this method is based on the premise that the brain regions transiently interact with each other during periods of cognitive activity (Bastos et al., 2015;

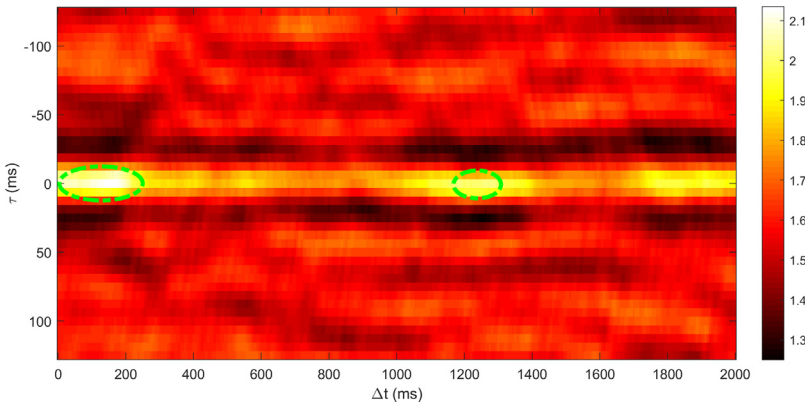

Fig. 12. The illustration of the average synchronization values between FP2-F8 channels calculated for each $\{\Delta t, \tau\}$ combination for right fist motor imagery activity. The green ellipse represents the candidate maximal synchronization patterns. We used cosine similarity method to calculate the synchronization values of subject S004 who elicited the most successful recognition performances for the PhysioNet Motor Movement/Imagery dataset.

Table 5
The activity-specific timing parameter triplets obtained during scenario-2 using linearized mutual information metric for CCP5-CP3 channel pair for right foot and F3-CFC3 during right hand motor imagery activity (BCI Competition-III dataset IVa).

Subject ID	Right foot imagery activity-specific timing parameter (CCP5-CP3)			Right hand imagery activity-specific timing parameter (F3-CFC3)			Performance (at Scenario-2)
	Δt (ms)	τ (ms)	w (ms)	Δt (ms)	τ (ms)	w (ms)	
aa	1590	0	520	220	0	580	**67.39%**
al	1540	0	620	580	0	960	**91.30%**
av	800	0	560	360	0	550	**60.86%**
aw	1280	0	450	1730	0	570	**73.91%**
ay	770	0	360	1460	0	820	**89.13%**

Table 6
The activity-specific timing parameter triplets obtained during scenario-2 using linearized mutual information for FPz-FT7 channel pair for left fist motor imagery activity and for FP2-F8 during right fist motor imagery activity (PhysioNet Motor Movement/Imagery dataset). We used the most successful 8 subjects that elicited more than **64%** performance (Müller-Putz et al., 2007).

Subject ID	Left fist imagery activity-specific timing parameter (FPz-FT7)			Right fist imagery activity-specific timing parameter (FP2-F8)			Performance (at Scenario-2)
	Δt (ms)	τ (ms)	w (ms)	Δt (ms)	τ (ms)	w (ms)	
S001	0	0	563	0	0	518.8	**73.33%**
S002	1912	0	387.5	31.3	0	493.8	**80%**
S004	31	6.25	462.5	0	−6.25	500	**86.67%**
S006	231	0	575	0	0	818.8	**73.33%**
S007	0	0	493.8	0	0	650	**73.33%**
S015	118.8	0	487.5	12.5	0	662.5	**86.87%**
S018	0	0	512.5	0	−6.25	443.8	**80%**
S020	225	−6.25	462.5	12.5	−6.25	431.3	**73.33%**

Fries, 2005). These reciprocal interactions may carry critical neural information which is vital for the generation of task-specific neural patterns within the brain. In our previous study, we calculated only the synchronization lags (τ) between the channel pairs which was found to be useful for characterizing the cognitive activity (Olcay & Karaçalı, 2019). However, according to Bastos et al. and Fries et al. the activity-specific inter-regional interactions emerge and vanish in relatively short time intervals within the task periods. In order to track this behavior, in this study, we extended our earlier approach with the addition of two new timing parameters (i.e., the latency of maximal synchronization between channel pairs from activity onset (Δt), and duration of maximal synchronization among channel pairs (w)) to characterize the cognitive activities.

Since we do not know which synchronization measure would capture the actual neural synchronization patterns that emerge within the brain better, we tried six different synchronization measures and evaluated their performance in a motor imagery activity recognition framework. The reason for using these synchronization measures is that they elicited a better characterization performance in the past literature and that they had favorable computational properties. In the literature, there are many additional synchronization methods that have been used in various types of brain activity characterization studies. We believe that the six measures we have evaluated in our study covers the range of prominent and effective similarity measures well.

Lastly, the majority of brain activity characterization studies in the literature use the entire task periods to calculate connectivity-based features. As depicted above, there is evidence in the literature that the task-related information is embedded within the signal pairs only for a limited duration. These finite-length signal pairs can thus be used to calculate several features such as common spatial patterns (CSP), power-based features, time domain features … etc. to further improve task recognition performances.

In the light of these motivations, our method presented in this paper captures the activity-specific timing parameter triplets of the characteristic short-lived synchronization between EEG channels for each channel pair and each cognitive activity type. In order to determine the activity-specific timing parameter triplets, we adopted a heuristic search method that uses a 300ms-length sliding time window to calculate average channel synchronizations across all task periods for the remaining delay parameter combinations. We then evaluated the usefulness of the channel synchronizations calculated at activity-specific timing parameter triplets in a motor imagery task recognition setting and in statistical tests comparing the resulting synchronizations between the contending cognitive tasks. Prior to the classification, we selected the most discriminative synchronization features for a better classification. We observed that, for both dataset, both adjacent and non-adjacent channel pairs remained after the feature selection which is in line with the fact that many different brain regions are involved to integrate information during cognitive tasks (Mišić & Sporns, 2016; Telesford et al., 2011; Uhlhaas et al., 2009). The recognition performances and the statistical test results reveal several insights on connectivity based brain activity characterization as discussed below.

4.1. Performance evaluation and comparison

The average recognition performances obtained for six different synchronization metrics for both BCI Competition-III (right-foot/right-hand imagery) and PhysioNet (right-fist/left-fist imagery) in Figs. 5 and 6 show that the linear mutual information and cosine-based similarity methods demonstrated the top-ranking average performances in scenario-2 for BCI Competition-III and PhysioNet datasets, respectively. This outcome indicates that these two synchronization metrics capture the timings of the characteristic synchronizations of the channel pairs more accurately than the other methods used in this study.

In terms of recognition performances, the CSP-based method ranked supreme on the BCI Competition-III dataset IVa as expected since a CSP-based approach was the winner of the competition. On the PhysioNet dataset, the proposed method surpasses the CSP recognition performance which suggests that the CSP method may be overfitted to the BCI Competition data and may not necessarily do as well in other instances. In comparison, the performance of the proposed method was more stable on both datasets. The univariate AR model based method, however, did not perform well despite its popularity in the literature.

Note that the most likely reason for performances lower than the minimum reliable communication rate of 70% on the PhysioNet dataset may be the small number of task periods considering that even 30 task periods for training in scenario-2 may be insufficient to extract reliable average synchronization patterns (Ahn & Jun, 2015). In the specific case of CSP these results suggest that the method could not find suitable spatial filters to discriminate between different cognitive activities due to inaccurate estimates of spatial covariance matrices.

Another possible reason for low performances on the PhysioNet dataset may be a low signal-to-noise ratio. In the literature, the studies that employ the PhysioNet dataset, in general, use noise/artifact removal methods to filter out the non-neural signals (Varsehi & Firoozabadi, 2021). In such a case, it may be helpful to use various denoising techniques in the preprocessing step to identify and remove the noise component from the EEG signals (Hyvärinen & Oja, 2000; Jolliffe, 1986; Von Bünau et al., 2009). Despite these problems, it is noteworthy that the proposed method achieved the best performance among the four competing approaches on the PhysioNet dataset, indicating robustness against various pitfalls associated with changes in EEG procedures, equipment, or signal recording quality. Importantly, in the literature, the majority of the motor imagery activity recognition studies on the PhysioNet dataset report the performance results of only the well-performing subjects with recognition performances over 64% (Athif & Ren, 2019; Handiru & Prasad, 2016; Kim et al., 2016; Park et al., 2014; Tolić & Jović, 2013). In this study, we showed the average performances of the first 20 subjects without any performance-related elimination criteria to clarify the pros and cons of the proposed method along with the alternative techniques.

4.2. The effect of window size

Our heuristic optimization method uses a 300ms-length time window as an initial step of the procedure used to obtain the timing parameter triplets associated with the characteristic pairwise channel synchronizations. For the BCI Competition-III dataset IVa ($f_s = 100$ Hz), this corresponds to 30 samples and for the PhysioNet dataset ($f_s = 160$ Hz), to 48 samples for synchronization calculations. Using such low number of samples, however, especially for BCI Competition-III dataset IVa, may lead to an underestimation of synchronization (Fraschini et al., 2016; Sideridis et al., 2014). This suggests that using an EEG recording system with a greater sampling frequency may improve the resolution with which the optimal timing parameters are determined and increase the number of samples in the 300ms-length time window for more accurate synchronization estimates.

4.3. Biophysical relevance of the identified channel pairs

We identified the most significant channel pairs according to the geometric means of the corrected P-values of the pairwise channel synchronizations calculated at activity-specific timings obtained for both datasets in scenario-2. For the BCI Competition-III dataset IVa, the most significant channel pairs for more accurate synchronization estimates for right foot motor imagery task correspond to the left central and left centro-parietal electrode pairs CCP5-CP3 ($P < 0,001$), C3-CCP3 ($P < 0,001$), and C5-CCP5 ($P < 0,001$). As for right hand motor imagery task, the most significant channel pairs include left frontal, left fronto-central and left central electrodes/electrode pairs F3-CFC3 ($P < 0,001$), FFC3-FCF3 ($P < 0,001$), and FC1-C3 ($P < 0,001$). We also provided the resulting P-values for all channel pairs of BCI Competition-III dataset IVa as supplementary materials. These results suggest that the majority of the electrodes that elicit significant task-specific synchronization across all 5 subjects are mainly located on the left hemisphere, which is consistent with the existing literature (Chen et al., 2019; Chung et al., 2011; Gao et al., 2011; Gonuguntla et al., 2016; Halder et al., 2011; Hanakawa, 2016; Hétu et al., 2013; Höller et al., 2013; Kasess et al., 2008; Munzert et al., 2009; Pfurtscheller & Berghold, 1989; Pfurtscheller & Neuper, 1997; Xu et al., 2014).

As for the PhysioNet dataset, we obtained the top three most frequently observed significant channel pairs according to the geometric means of P-values of the channel synchronizations for the first 20 subjects. For left fist motor imagery activity, the electrodes associated with these channel pairs are generally placed on the left frontal, left fronto-temporal, and left temporal regions. Similarly, for the right fist imagery activity, the significant electrodes are placed on right and left frontal and right frontal as well as temporal regions, respectively. Although these findings fall at odds with the current biophysical literature on the right/left hand motor imagery activity that points to the significance of the contralateral connectivity patterns during motor imagery tasks, there are several important biophysical studies that found ipsilateral activations/synchronization profiles as significant (Brunner et al., 2006; Gao et al., 2011; Kraeutner et al., 2014; Porro et al., 2000), especially for the novice participants (Milton et al., 2007).

The emergence of ipsilateral synchronization patterns falls between frontal/fronto-temporal electrodes during motor imagery tasks might be due to several reasons. First, there may be an excessive information flow from parietal to frontal regions to compensate for the imagination inability during kinesthetic motor imagery task which may cause unexpected short-lived synchronization (Bauer et al., 2015; Gu et al., 2020; Menicucci et al., 2020). Another reason may be the insufficient number of training task periods available for statistical analysis: in the PhysioNet dataset, there are only 45 motor imagery activity task periods in total for each subject which may cause subject-specific inter-regional synchronization (Demuru & Fraschini, 2020; Pani et al., 2020; Xie et al., 2018). By filtering the subject-specific synchronization modulations or using a greater number of motor imagery task periods, more reliable and biophysically relevant channel pairs may be expected to emerge (Allen et al., 2014).

Furthermore, the frontal channel synchronizations observed on the PhysioNet dataset may be the result of an inherent condition of the human brain: if the participants' "mind sets" cannot be fully isolated from internal (e.g., concentration, focusing momentarily on other issues, some accompanying thoughts,

etc.) or external (any minor external trigger etc.) factors, the inferred electrophysiological organization of the brain may alter substantially. Furthermore, a change of the imagination strategy such as from kinesthetic imagery to visual imagery or vice versa by the participants during the task may significantly modify the information processing scheme and thus the inter-regional synchronization timings of the brain that causes a performance deterioration (Neuper et al., 2005; Park et al., 2015).

4.4. The effect of time lag on characterization performance

We presented sample synchronization patterns observed for different subjects during the heuristic optimization scheme to determine the optimal timing parameter triplets in Figs. 9–12. Interestingly, these figures along with the timing parameters (see Tables 5 and 6) show that the short-lived synchronization patterns emerge and vanish at different timings, but more importantly, the time lag between the corresponding signal segments of the most significant channel pairs is near or exactly equal to zero. This shows a zero-lag organization between primarily activity-related regions potentially to integrate the neural information into coherent representational states which provides effective as well as efficient information transfer during a cognitive task (Roelfsema et al., 1997). The zero-lagged synchronization may also be the result of an organization mechanism that dynamically relays the neural information among the activity-related regions via thalamo-cortical circuit and/or hippocampal circuits (Vicente et al., 2008).

The channel pairs that we identified as the most significant for BCI Competition-III dataset IVa (CCP5-CP3 for right foot activity, and F3-CFC3 for right hand activity), and for PhysioNet Motor Movement/Imagery dataset (FPz-F7 for left fist activity, and FP2-F8 for right fist activity) are relatively close to each other as demonstrated in Fig. 13. Since the aforementioned electrodes are placed relatively close to each other, they tend to collect the electrophysiological activities from overlapping cortical structures. In this circumstance, the most probable reason why the time lag between these channel pairs is near or equal to zero for each subject is the volume conduction problem which hampers the actual time lag between these channel pairs (Bastos & Schoffelen, 2016; Tognoli & Kelso, 2009). To minimize the effects of volume conduction, we used the common average referencing (CAR) method before the synchronization calculation (McFarland et al., 1997; Tsuchimoto et al., 2021). However, as Cohen stated, there is no perfect method that completely eliminates the effects of volume conduction (Cohen, 2015). In order to achieve a slightly better characterization performance, more advanced spatial filtering techniques are required albeit with a greater computational cost (Rathee et al., 2017).

Although the volume conduction appeared as the primary reason, we actually do not know the exact timings (Δt, τ, and w) of the activity-specific synchronization for each channel pair. In our results, we observed zero-lagged short-lived synchronization for the most significant channel pair which is not necessarily completely due to volume conduction phenomena. For instance, Witham et al. observed in the monkeys that the movement-related cortical synchronization between relatively close areas emerges at zero time lag (Witham et al., 2007).

It is important to highlight that, not all channel pairs synchronize at zero time lag. The channel pairs presented in Tables 5 and 6 in the manuscript, were the most statistically significant in terms of their short-lived interactions (as the result of t-tests), and also, these channels are the one of most frequently selected channel pairs as features (according to the Fisher ratio) for each activity type. In addition to these channel pairs, there are also other channel pairs that elicit significant synchronization with an inter-channel time lag different from zero.

Table 7
The electrode clusters of BCI Competition-III dataset IVa and PhysioNet dataset according to CB2 subset. This clusters contain C3, C4, and Fz channels and their nearest neighbors.

Cluster-1	Cluster-2	Cluster-3
Fz	C3	C4
AF3	FC3	FC4
AF4	CP3	CP4
F1	C5	C6
F2	C1	C2
FCz	–	–

We performed an extra analysis and observed that not only adjacent but also non-adjacent channels may elicit zero-lag synchronization. We used several channel pairs that were used in previous motor imagery activity recognition studies. We determined the activity-specific timings of these channel pairs for each different cognitive activity, and we calculated the channel synchronizations to use in a motor activity recognition framework. In a previous synchronization-based motor imagery activity characterization study, both adjacent and non-adjacent channel pairs were used (Wei et al., 2007). In that study, the channels Fz and its neighbors (Cluster-1), C3 and its neighbors (Cluster-2), and C4 and its neighbors (Cluster-3) achieved the best recognition accuracy. These electrodes are known to collect the electrophysiological activity from left and right primary motor, sensorimotor, premotor and prefrontal cortices which are actively engaged in motor imagery tasks (Chung et al., 2012; Decety, 1996; Munzert et al., 2009). We paired the channels (i.e., Cluster-1 ↔ Cluster-2, Cluster-1 ↔ Cluster-3, and Cluster-2 ↔ Cluster-3) contained in different clusters without considering the intra-cluster channel pairs, providing a total of 85 non-adjacent channel pairs (please see Table 7 for the channels). Please note that since the EEG recording system that was used to collect BCI Competition-III dataset IVa did not contain the AFz electrode, we included both AF3 and AF4 electrodes instead of AFz.

We showed the time lags of the channel synchronizations for each of the 85 pairs during right hand motor imagery activity in Fig. 14. Note also that, for synchronization calculation, we used linear MI which appeared as the most successful measure for BCI Competition-III dataset IVa on the average. The "*" symbol above/below the time lag bars indicates that the timing parameter triplet elicited statistically significant synchronization for that channel pair for right hand motor imagery activity.

We repeated the time lag estimation for the correntropy method for the subject *al* for which we observed the highest performance (93,47%). We showed the correntropy results in Fig. 15.

In these figures, it is clear that not only the adjacent channel pairs synchronized at zero lag but also several non-adjacent channel pairs significantly synchronized at zero-lag along with several other pairs for which activity-specific synchronization occurred at non-zero time lags.

In addition to the above analysis, we obtained 1452 pairwise short-lived synchronizations as significant. Among these synchronizations 391 of them demonstrated non-zero time lag for linear mutual information method. Furthermore, for the correntropy method, out of the 1757 significant pairwise synchronizations, 1017 of them demonstrated non-zero time lag. These results point that the main source of lag between the EEG signals as identified by the synchronization measure of choice is the delay between electrophysiological signals generated by the brain during cognitive tasks according to a timing organization (Hari & Parkkonen, 2015).

This shows that the brain adjusts the timings of the synchronizations according to the task demands in the associated

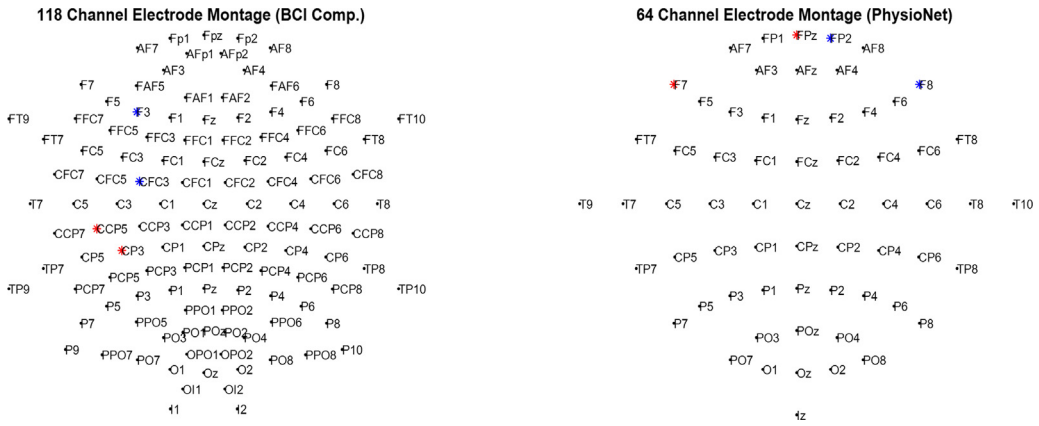

Fig. 13. Illustration of the electrode montages of both PhysioNet and BCI Competition-III dataset IVa. The electrodes that marked with red star was found as significant channel for one cognitive activity, and the electrodes marked with blue star was found as significant for another cognitive activity. (For interpretation of the references to color in this figure legend, the reader is referred to the web version of this article.)

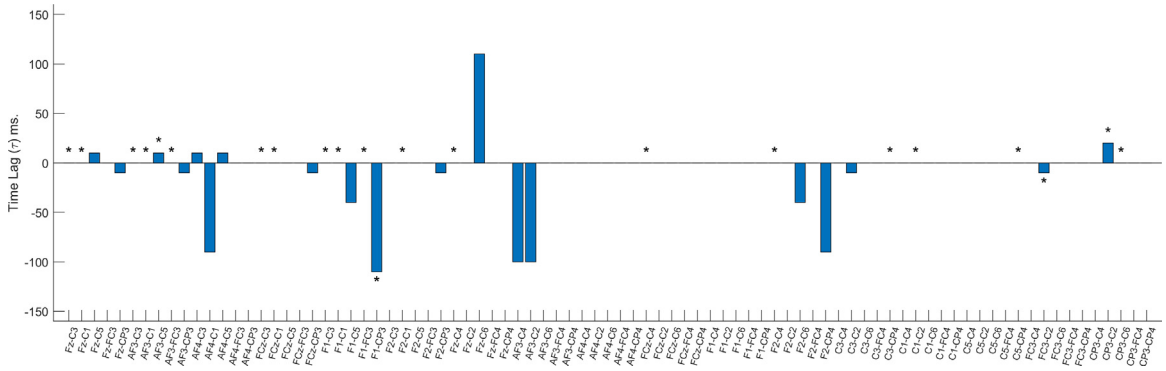

Fig. 14. The illustration of time lag parameters for short-lived synchronization of non-adjacent channels for right hand motor imagery activity for subject *al* (for linear MI). Note that the '*' symbol above or below the lag representation bar plots denotes that the synchronization of corresponding channel pair is statistically significant ($P < 0.05$).

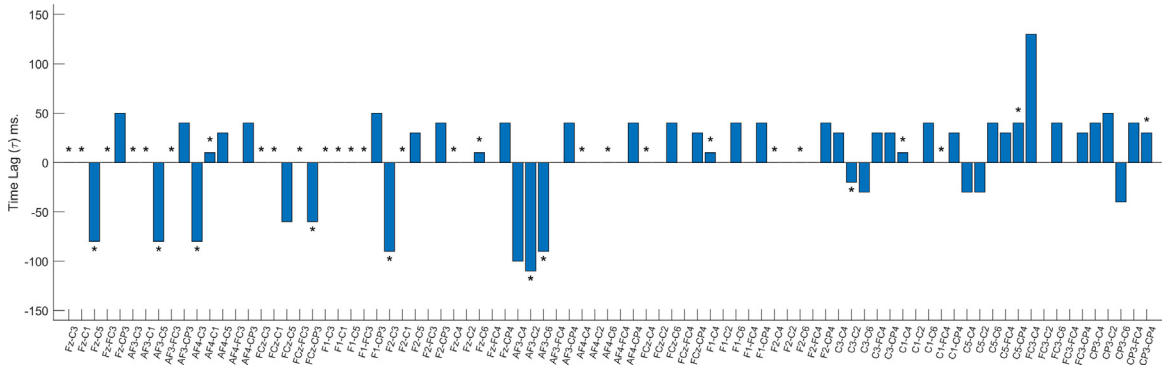

Fig. 15. The illustration of time lag parameters for short-lived synchronization of non-adjacent channels for right hand motor imagery activity for subject *al* (for correntropy). Note that the '*' symbol above or below the lag representation bar plots denotes that the synchronization of corresponding channel pair is statistically significant ($P < 0.05$).

regions with communication through hypothesis. This hypothesis suggests that the brain generates temporal communication windows by maximizing the temporal synchronization among its regions for task-specific neural information transfer (Bastos et al., 2015; Fries, 2005). These inter-areal communication windows integrate the processed segregated information. We observed that the timings of the short-lived maximal synchronization elicited significantly different synchronizations for different types of motor imagery activities. The differences of the timing parameters triplets are thought to be the result of different neural mechanisms taking place for different activities. In Gao et al. (2019), it was demonstrated that neural synchronizations calculated at normal conditions show a significant difference when calculated in a fatigue mood. This shows that neuronal conditions exhibit significant alteration between different brain states, and this alteration affects the neural synchronization dynamics. In a similar vein, Salyers et al. showed that different task conditions requires different network coordination (Salyers et al., 2019).

There are other studies in the literature that point to the systematic time lag organization between brain regions (Adhikari et al., 2010; Bastos et al., 2015; Mijalkov et al., 2020; Olcay &

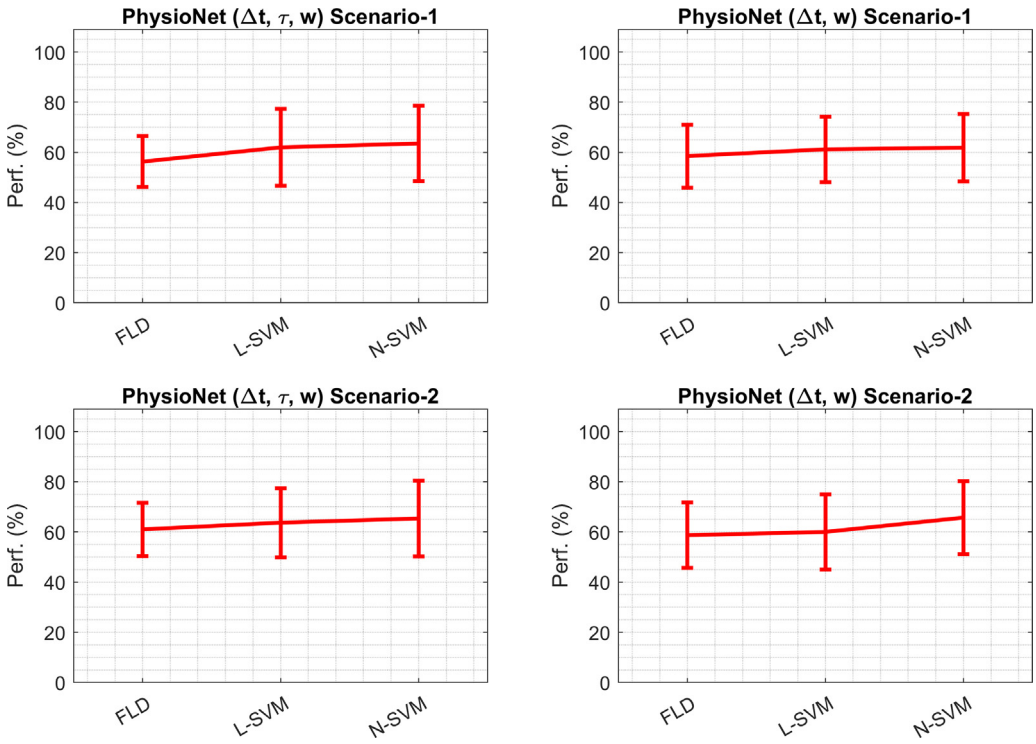

Fig. 16. The average recognition performance obtained under a universal zero-lag assumption indicated by $\{\Delta t, \tau\}$ in comparison with the proposed method for PhysioNet dataset.

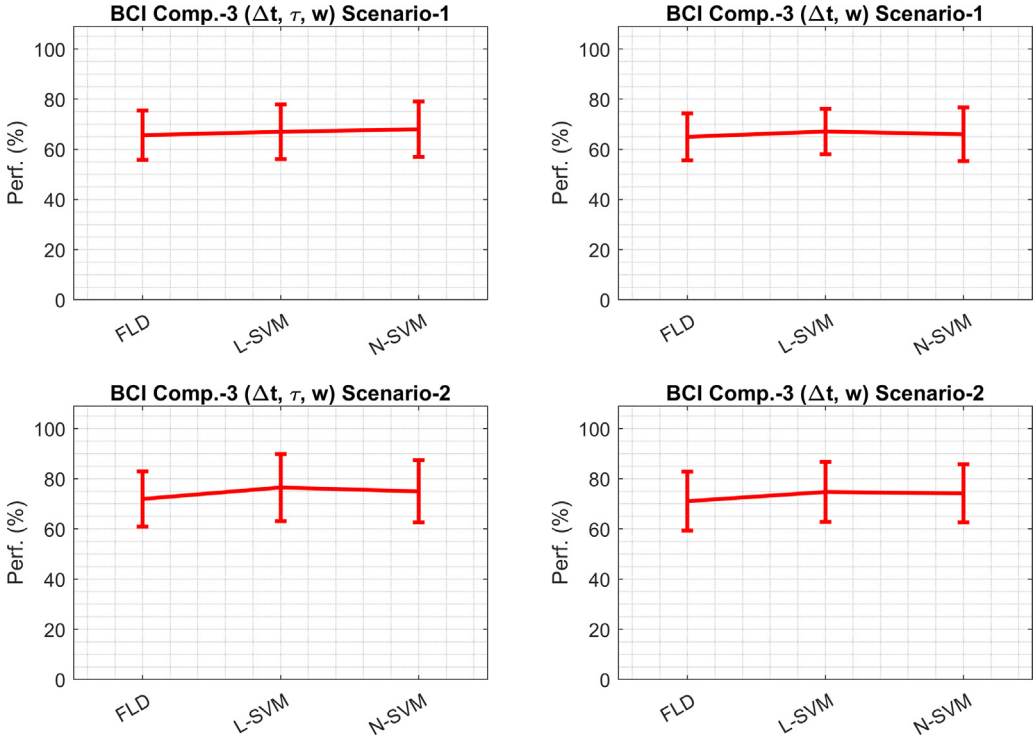

Fig. 17. The average recognition performance obtained under a universal zero-lag assumption indicated by $\{\Delta t, \tau\}$ in comparison with the proposed method for BCI Competition-III dataset.

Karaçalı, 2019). In order to determine the effect of the zero-lag assumption on the activity recognition performance, we conducted another classification analysis where we set $\tau = 0$ and optimized the average inter-channel synchronizations with respect to Δt and w only for each channel pair and each type of motor imagery activity. The performance results presented in Figs. 16 and 17 shows that the recognition accuracy obtained using the proposed $\{\Delta t, \tau, w\}$-based method is, in general, greater than the performances obtained by assuming a zero time lag. The findings of statistical comparison tests clearly establish that maximal task-specific synchronizations often occur at non-zero time-lags, albeit with minor improvements in the overall task recognition

performance. A possible explanation for some low performances presented in Figs. 16 and 17 is the relatively stronger reliance of the classifiers to the channel pairs with zero time lag, limiting the effects of channel pairs with non-zero time lag on the task recognition performance. In a more intriguing scenario, however, this may also be due to the fact that the proposed three-parameter representation for the task-specific synchronization fails to adequately account for inter-trial variations in subject task comprehension and response. We are currently in the process of expanding our formulation to cover such subject and trial specific effects on task-specific channel synchronizations.

To sum up, the performance results presented in Figs. 16 and 17 suggest that not all brain regions synchronize at a zero-lag during cognitive tasks. In the same context, as pointed out in Qian et al. (2013), the time lag parameter is a crucial parameter that decides the characteristics of the neural functions. This outcome stresses the importance of considering time-lagged synchronization between brain regions in cognitive activity characterization applications.

4.5. Biophysical evidences for considering the latency and duration parameters

The electrophysiological activity obtained during controlled experiments show that the task related brain patterns from any external (or internal) stimulation would continue for hundreds of milliseconds (Bayazit et al., 2009; Güdücü et al., 2019; Olcay et al., 2017; Schack et al., 2003) (please see Tables 5 and 6). For instance, it was shown that during processing of internal and external stimuli, intra- and inter-hemispheric short-lived synchronizations may emerge in a temporal order to evaluate the complex nature of the stimulus (Bola et al., 2015; Solomon et al., 2019; Zanon et al., 2018). This shows that the bottom-up cognitive task related information processing is embraced with top-down higher-level content assessment. But more importantly, it signifies that the short-lived activations/synchronizations of different and distant brain regions in response to a stimulus or during a cognitive task may manifest according to a temporal order for efficient and effective brain coordination (Bullmore & Sporns, 2012; Dawson, 2004; Dimitriadis et al., 2013). In a previous BCI study, a similar strategy was adopted for feature extraction. J. Li et al. proposed to use time–frequency mask (TFM) to capture the discriminative time–frequency features embedded in a small time and frequency range (Li et al., 2016). This study highlights the importance of the time-sensitive feature analysis when characterizing the brain activities further. This supports that taking the latency (Δt) as well as the duration (w) parameters of the temporal information processing timings into account for the analysis of short-lived electrophysiological brain synchronizations.

As an important point, it was presented in Tables 5 and 6, the latency (Δt) and duration (w) parameters vary considerably across the subjects. According to the information provided by the two datasets that we used in our study; these subjects performed only motor imagery tasks associated with the command provided by the experimenter (Dornhege et al., 2004; Goldberger et al., 2000).

The variation of these parameters is thought to be due to the different mental strategies adopted by the subjects during these tasks (Friedrich et al., 2012; Kilintari et al., 2016). Differences in mental strategies among the subjects can be observed in the timing parameter triplets identified for each mental task and channel pair. Please note that the latency (Δt) and duration (w) parameters are thought to be indicators of temporal processing of the task-related information in the brain. The timing parameters (Δt, τ, and w) are systematically adjusted according to the mental strategies that the subjects adopt.

It is important to note that the subject's condition may also have a significant impact on these parameters in addition to the task requirements. Especially the latency Δt parameter is inevitably affected by several important factors such as the subject's command perception time, and initialization time to motor imagination, which may cause random variations from trial to trial during motor imagery tasks.

Our reasoning in seeking the optimal timing parameters using the average synchronization values is based on the premise that since perception and task initiation are subjective parameters and vary randomly according to the aforementioned reasons, averaging of synchronization values ought to minimize these task-unspecific (i.e., subject-specific) variations and allow capturing the task-specific timing parameters. The performance results, which we presented in the manuscript, show that, especially in scenario-2 that uses a greater number of training task periods, we elicited a better recognition performance than obtained in scenario-1.

4.6. Alternative synchronization metrics

In this study, we evaluated six different synchronization measures to identify the timings of the short-lived characteristic channel synchronizations. The choice of these similarity measures was made in part due to their computational efficiency, along with their favorable performances observed in past studies including our own previous work Olcay and Karaçalı (2019) and in Zalesky et al. (2012). The differences observed in the recognition performances for each metric (please see Figs. 5–8) are due to the differences in the way synchronization is evaluated by the methods: Each method extracts and uses a different aspect of the signal features to calculate channel synchronizations (Sakkalis, 2011).

Alternative measures can also be used such as phase lag index (PLI) (Stam et al., 2007), imaginary part of coherency (imCOH) (Nolte et al., 2004), transfer entropy (TE) (Schreiber, 2000; Wibral et al., 2013, 2014), coherence (COH) (Bakhshayesh et al., 2019a; Greenblatt et al., 2012; Rocca et al., 2014; Sakkalis, 2011; Wendling et al., 2009), cross-sample entropy (Gomez et al., 2016), and synchronization likelihood (Stam & Van Dijk, 2002). This study can also be conducted via Kraskov's mutual information estimation method (Kraskov et al., 2004) which elicited the best performance in our previous study (Olcay & Karaçalı, 2019). However, mutual information calculation between the signal segments across the whole datasets via Kraskov's method is computationally prohibitive. Advanced parallel computing architectures coupled with efficient algorithms can be investigated to overcome the computation issues of Kraskov's mutual information estimation.

4.7. Future directions for brain–computer interface systems

As for the potential extension of the methodology proposed here to brain–computer interfacing applications, it should be noted that the core of the method relies on identifying the channel pairs with significantly different synchronization characteristics during different activities in terms of optimal activity-specific timing parameters. Clearly, once the activity-specific timing parameter triplets of the characteristic pairwise channel synchronizations are identified, the synchronizations can be used as features in a connectivity-based BCI framework. First and foremost, filtering of the EEG signals into 8–30 Hz frequency band is consistent with many BCI studies where the motor imagery related information is sought within the frequency range of 8–30 Hz (Lafleur et al., 2013; McFarland & Wolpaw, 2008; Yuan &

He, 2014). Several studies used a filter-bank structure or wavelet-based methods for brain activity characterization (Emre Cek et al., 2010; Higashi & Tanaka, 2013; Kumar et al., 2017; Nguyen-Ky et al., 2012; Park et al., 2018; Rosso et al., 2001, 2006). Clearly, a filter-bank strategy or a discrete wavelet transform analysis may also be incorporated here prior to the synchronization calculation, allowing analysis of different frequency bands (Ang et al., 2008; Park et al., 2018; Walden & Contreras Cristan, 1998). For instance, the importance of μ and β band networks during motor imagery activity was revealed in earlier studies (Athanasiou et al., 2018; Gu et al., 2020). Also, the μ rhythm dynamics have been associated with the motor imagery related information processing among the motor cortical regions (Başar et al., 2001; Llanos et al., 2013). However, it should be noted that an increase in the spectral resolution using wavelet-based or filter bank-based methods entails a substantial increase in computational cost, requiring repeated calculations for each frequency band.

As an extension, our method can reliably be considered in human–computer interaction such as gesture recognition applications. Up to now, many different conspicuous efforts have been spent to increase the accuracy of gesture recognition applications (Li, Li et al., 2019; Sun et al., 2020). In this respect, brain synchronization/activation features can additionally be adopted to increase the recognition accuracy. Once the important EEG channel pairs and the corresponding movement-specific inter-regional synchronization timings are determined in training phase, our method can reliably be used in conjunction with current surface EMG-based gesture recognition methods to achieve improved movement identification performances and thus be used in hand motion controlled devices. In a similar manner, the proposed timing-based brain activity analysis method can also be used to detect brain lesions, which may cause significant alterations of inter-regional communication patterns (Li, Jiang et al., 2019).

On a final note, it should be emphasized that, the approach presented here deviates significantly from the majority of the brain activity characterization studies in the literature that aim to extract characteristic synchronization-based features for different motor imagery tasks using whole activity periods (Anderson et al., 1998; Feng et al., 2018; Lemm et al., 2005). Notably, a critical issue can arise when using the whole activity periods to determine activity-specific brain patterns: Although the exact time of initiation and end cue for motor imagery activity is known in synchronous BCI experiments, the initiation and end time of the reciprocal information processing can be different for different brain regions (Curran & Stokes, 2003). That means the activity-related localized activation/synchronization dynamics may emerge and disappear in a short period of time due to the activity-specific timing organization. In the literature, few studies attempt to find the most informative short-lived time segment (Ang et al., 2012; Hsu et al., 2007; Wang et al., 2018, 2020; Zhang et al., 2019). These studies, however, used time windows of fixed duration, usually 1 or 2 s, disregarding potential variations in the duration of the brain's responses. In our study, optimal latency (Δt), time lag (τ) and duration (w) of the coupling were determined to capture activity-specific inter-channel synchronization for each motor imagery activity type and each channel pair, addressing both issues listed above to their full complexity.

5. Conclusion

The brain appears to operate through multi-dimensional states (Breakspear & Stam, 2005). Communication among different regions, sensory and motor information processing associated areas, and frontal/prefrontal areas co-exist. The nature of asymmetrical brain response to dichotic stimulus has given some insight to trans-hemispheric and posterior-frontal axes in stimulus-specific time intervals (Bayazit et al., 2009). The operational complexity as well as the timing specialization of the brain forces us to seek novel analysis methods that can elucidate the characteristic as well as transient synchronization between distinct brain regions. Since cognition as well as other processes shows nonstationary behavior, methods that invoke stationarity assumptions on brain electrophysiology are rendered inadequate to reveal the characteristic synchronization.

The major shortcoming of the classical analysis methods is the disregard of the transient as well as the complex nature of the brain's distributed functionality in favor of model simplicity. The more adequate distributed systems approach requires new tools as the function blocks are widely distributed and the information complexity overwhelms locality to a large degree. This manuscript proposes a new framework that can be useful to trace and characterize the behavior of distributed information processing during cognition.

The methodology proposed here determines the timings of the characteristic synchronizations among the brain structures for different cognitive activities. The differences in the timings for each different cognitive activity and each different brain region indicate that the brain generates transient synchronization windows to integrate the segregated neural information to support a rich variety of cognitive processes (Zalesky et al., 2014). Additionally, these differences in the synchronization timings may constitute a "synchrony filter" to inhibit the interference of task-unspecific neural synchronizations coming from different brain regions (Patel & Joshi, 2013). The cognitive task recognition performance results point to the importance of considering time-resolved cortical communication for discovering the working principles of the brain.

To conclude, in this study:

- We adopted the temporal communication-through-coherence perspective for motor imagery activity characterization that uses inter-areal time delays as Bastos et al. suggested (Bastos et al., 2015). We determined the timing organization among the brain regions and used them for cognitive activity characterization.
- As previously demonstrated in Ince et al. (2009) and Li et al. (2016) the accurate brain activity characterization requires a time-sensitive analysis to extract task-related features. In a similar vein, we show that an accurate brain activity characterization requires temporal synchronization analysis.
- Our analysis extended the premise that the brain synchronization emerges at similar time lags for similar cognitive activities (Bandt et al., 2019; Feige et al., 2017; Hermanto et al., 2013; Mitra et al., 2015). Here, we showed that the brain exhibits synchronization patterns not only on specific time lags but also at specific latency and duration parameters as well. In this context, we have relaxed the common brain activity characterization assumptions adopted by popular methods such as CSP adopt, associated with implicit assumption of zero lag and zero latency and which uses entire task period to extract relevant brain dynamics.

Declaration of competing interest

The authors declare that they have no known competing financial interests or personal relationships that could have appeared to influence the work reported in this paper.

Acknowledgment

This study was supported by a grant awarded to Dr. Bilge Karaçalı by The Scientific and Technological Research Council of Turkey (TUBITAK) with grant number 117E784.

Appendix A. Supplementary data

Supplementary material related to this article can be found online at https://doi.org/10.1016/j.neunet.2021.06.022.

References

Abiri, R., Borhani, S., Sellers, E. W., Jiang, Y., & Zhao, X. (2019). A comprehensive review of EEG-based brain-computer interface paradigms. *Journal of Neural Engineering*, *16*(1), 11001. http://dx.doi.org/10.1088/1741-2552/aaf12e.

Adhikari, A., Sigurdsson, T., Topiwala, M. A., & Gordon, J. A. (2010). Cross-correlation of instantaneous amplitudes of field potential oscillations: A straightforward method to estimate the directionality and lag between brain areas. *Journal of Neuroscience Methods*, *191*(2), 191–200. http://dx.doi.org/10.1016/j.jneumeth.2010.06.019.

Ahn, M., & Jun, S. C. (2015). Performance variation in motor imagery brain-computer interface: A brief review. *Journal of Neuroscience Methods*, *243*, 103–110. http://dx.doi.org/10.1016/j.jneumeth.2015.01.033.

Alais, D., Blake, R., & Lee, S. H. (1998). Visual features that vary together over time group together over space. *Nature Neuroscience*, *1*(2), 160–164. http://dx.doi.org/10.1038/414.

Allen, E. A., Damaraju, E., Plis, S. M., Erhardt, E. B., Eichele, T., & Calhoun, V. D. (2014). Tracking whole-brain connectivity dynamics in the resting state. *Cerebral Cortex*, *24*(3), 663–676. http://dx.doi.org/10.1093/cercor/bhs352.

Ambrosi, P., Costagli, M., Kuruoglu, E. E., Biagi, L., Buonincontri, G., & Tosetti, M. (2019). Investigating time-varying brain connectivity with functional magnetic resonance imaging using sequential Monte Carlo. In *European signal processing conference*, *2019-Septe* (pp. 1–5). http://dx.doi.org/10.23919/EUSIPCO.2019.8902503.

Anderson, C. W., Stolz, E. A., & Shamsunder, S. (1998). Multivariate autoregressive models for classification of spontaneous electroencephalographic signals during mental tasks. *IEEE Transactions on Biomedical Engineering*, *45*(3), 277–286. http://dx.doi.org/10.1109/10.661153.

Ang, K. K., Chin, Z. Y., Zhang, H., & Guan, C. (2008). Filter bank common spatial pattern (FBCSP) in brain-computer interface. In *Proceedings of the international joint conference on neural networks* (pp. 2390–2397). http://dx.doi.org/10.1109/IJCNN.2008.4634130.

Ang, K. K., Chin, Z. Y., Zhang, H., & Guan, C. (2012). Mutual information-based selection of optimal spatial–temporal patterns for single-trial EEG-based BCIs. *Pattern Recognition*, *45*(6), 2137–2144. http://dx.doi.org/10.1016/j.patcog.2011.04.018.

Arnold, M., Miltner, W. H. R., Witte, H., Bauer, R., & Braun, C. (1998). Adaptive AR modeling of nonstationary time series by means of kaiman filtering. *IEEE Transactions on Biomedical Engineering*, *45*(5), 545–552. http://dx.doi.org/10.1109/10.668739.

Athanasiou, A., Klados, M. A., Styliadis, C., Foroglou, N., Polyzoidis, K., & Bamidis, P. D. (2018). Investigating the role of alpha and beta rhythms in functional motor networks. *Neuroscience*, *378*, 54–70. http://dx.doi.org/10.1016/j.neuroscience.2016.05.044.

Athif, M., & Ren, H. (2019). Wavecsp: a robust motor imagery classifier for consumer EEG devices. *Australasian Physical and Engineering Sciences in Medicine*, *42*(1), 159–168. http://dx.doi.org/10.1007/s13246-019-00721-0.

Baker, A. P., Brookes, M. J., Rezek, I. A., Smith, S. M., Behrens, T., Smith, P. J. P., & Woolrich, M. (2014). Fast transient networks in spontaneous human brain activity. *ELife*, *2014*(3), http://dx.doi.org/10.7554/eLife.01867.

Bakhshayesh, H., Fitzgibbon, S. P., Janani, A. S., Grummett, T. S., & Pope, K. J. (2019a). Detecting connectivity in EEG: A comparative study of data-driven effective connectivity measures. *Computers in Biology and Medicine*, *111*, Article 103329. http://dx.doi.org/10.1016/j.compbiomed.2019.103329.

Bakhshayesh, H., Fitzgibbon, S. P., Janani, A. S., Grummett, T. S., & Pope, K. J. (2019b). Detecting synchrony in EEG: A comparative study of functional connectivity measures. *Computers in Biology and Medicine*, *105*, 1–15. http://dx.doi.org/10.1016/j.compbiomed.2018.12.005.

Bandrivskyy, A., Bernjak, A., McClintock, P., & Stefanovska, A. (2004). Wavelet phase coherence analysis: Application to skin temperature and blood flow. *Cardiovascular Engineering*, *4*(1), 89–93. http://dx.doi.org/10.1023/B:CARE.0000025126.63253.43.

Bandt, S. K., Besson, P., Ridley, B., Pizzo, F., Carron, R., Regis, J., Bartolomei, F., Ranjeva, J. P., & Guye, M. (2019). Connectivity strength, time lag structure and the epilepsy network in resting-state fmri. *NeuroImage: Clinical*, *24*(October), Article 102035. http://dx.doi.org/10.1016/j.nicl.2019.102035.

Başar, E., Başar-Eroglu, C., Karakaş, S., & Schürmann, M. (2001). Gamma, alpha, delta, and theta oscillations govern cognitive processes. *International Journal of Psychophysiology*, *39*(2–3), 241–248. http://dx.doi.org/10.1016/S0167-8760(00)00145-8.

Bashashati, A., Fatourechi, M., Ward, R. K., & Birch, G. E. (2007). A survey of signal processing algorithms in brain-computer interfaces based on electrical brain signals. *Journal of Neural Engineering*, *4*(2), R32–R57. http://dx.doi.org/10.1088/1741-2560/4/2/R03, IOP Publishing.

Bassett, D. S., Meyer-Lindenberg, A., Achard, S., Duke, T., & Bullmore, E. (2006). Adaptive reconfiguration of fractal small-world human brain functional networks. *Proceedings of the National Academy of Sciences of the United States of America*, *103*(51), 19518–19523. http://dx.doi.org/10.1073/pnas.0606005103.

Bastos, André M., & Schoffelen, J. M. (2016). A tutorial review of functional connectivity analysis methods and their interpretational pitfalls. *Frontiers in Systems Neuroscience*, *9*(JAN2016), 175. http://dx.doi.org/10.3389/fnsys.2015.00175.

Bastos, Andre M., Vezoli, J., & Fries, P. (2015). Communication through coherence with inter-areal delays. *Current Opinion in Neurobiology*, *31*, 173–180. http://dx.doi.org/10.1016/j.conb.2014.11.001.

Bauer, R., Fels, M., Vukelić, M., Ziemann, U., & Gharabaghi, A. (2015). Bridging the gap between motor imagery and motor execution with a brain-robot interface. *NeuroImage*, *108*, 319–327. http://dx.doi.org/10.1016/j.neuroimage.2014.12.026.

Bayazit, O., Öniz, A., Hahn, C., Güntürkün, O., & Özgören, M. (2009). Dichotic listening revisited: Trial-by-trial ERP analyses reveal intra- and interhemispheric differences. *Neuropsychologia*, *47*(2), 536–545. http://dx.doi.org/10.1016/j.neuropsychologia.2008.10.002.

Benjamini, Y., & Hochberg, Y. (1995). Controlling the false discovery rate: A practical and powerful approach to multiple testing. *Journal of the Royal Statistical Society. Series B. Statistical Methodology*, *57*(1), 289–300. http://dx.doi.org/10.1111/j.2517-6161.1995.tb02031.x.

Blankertz, B., Müller, K. R., Krusienski, D. J., Schalk, G., Wolpaw, J. R., Schlögl, A., Pfurtscheller, G., Millán, J. D. R., Schröder, M., & Birbaumer, N. (2006). The BCI competition III: Validating alternative approaches to actual BCI problems. *IEEE Transactions on Neural Systems and Rehabilitation Engineering*, *14*(2), 153–159. http://dx.doi.org/10.1109/TNSRE.2006.875642.

Blankertz, B., Tomioka, R., Lemm, S., Kawanabe, M., & Müller, K. R. (2008). Optimizing spatial filters for robust EEG single-trial analysis. *IEEE Signal Processing Magazine*, *25*(1), 41–56. http://dx.doi.org/10.1109/MSP.2008.4408441.

Boeijinga, P. H., & Lopes da Silva, F. H. (1989). A new method to estimate time delays between EEG signals applied to beta activity of the olfactory cortical areas. *Electroencephalography and Clinical Neurophysiology*, *73*(3), 198–205. http://dx.doi.org/10.1016/0013-4694(89)90120-X.

Bola, M., Gall, C., & Sabel, B. A. (2015). Disturbed temporal dynamics of brain synchronization in vision loss. *Cortex*, *67*, 134–146. http://dx.doi.org/10.1016/j.cortex.2015.03.020.

Bowyer, S. M. (2016). Coherence a measure of the brain networks: past and present. *Neuropsychiatric Electrophysiology*, *2*(1), 1–12. http://dx.doi.org/10.1186/s40810-015-0015-7.

Breakspear, M., & Stam, C. J. (2005). Dynamics of a neural system with a multiscale architecture. *Philosophical Transactions of the Royal Society, Series B (Biological Sciences)*, *360*(1457), 1051–1074. http://dx.doi.org/10.1098/rstb.2005.1643.

Brunner, C., Scherer, R., Graimann, B., Supp, G., & Pfurtscheller, G. (2006). Online control of a brain-computer interface using phase synchronization. *IEEE Transactions on Biomedical Engineering*, *53*(12), 2501–2506. http://dx.doi.org/10.1109/TBME.2006.881775.

Bullmore, E., & Sporns, O. (2012). The economy of brain network organization. *Nature Reviews Neuroscience*, *13*(5), 336–349. http://dx.doi.org/10.1038/nrn3214.

Burke, D. P., Kelly, S. P., De Chazal, P., Reilly, R. B., & Finucane, C. (2005). A parametric feature extraction and classification strategy for brain-computer interfacing. *IEEE Transactions on Neural Systems and Rehabilitation Engineering*, *13*(1), 12–17. http://dx.doi.org/10.1109/TNSRE.2004.841881.

Calhoun, V. D., Kiehl, K. A., & Pearlson, G. D. (2008). Modulation of temporally coherent brain networks estimated using ICA at rest and during cognitive tasks. *Human Brain Mapping*, *29*(7), 828–838. http://dx.doi.org/10.1002/hbm.20581.

Chaudhary, U., Birbaumer, N., & Ramos-Murguialday, A. (2016). Brain-computer interfaces for communication and rehabilitation. *Nature Reviews Neurology*, *12*(9), 513–525. http://dx.doi.org/10.1038/nrneurol.2016.113.

Chen, C., Zhang, J., Belkacem, A. N., Zhang, S., Xu, R., Hao, B., Gao, Q., Shin, D., Wang, C., & Ming, D. (2019). G-causality brain connectivity differences of finger movements between motor execution and motor imagery. *Journal of Healthcare Engineering*, (2019), http://dx.doi.org/10.1155/2019/5068283.

Chung, Y. G., Kang, J. H., & Kim, S. P. (2012). Correlation of fronto-central phase coupling with sensorimotor rhythm modulation. *Neural Networks*, *36*, 46–50. http://dx.doi.org/10.1016/j.neunet.2012.08.006.

Chung, Y. G., Kim, M. K., & Kim, S. P. (2011). Inter-channel connectivity of motor imagery EEG signals for a noninvasive BCI application. In *Proceedings - international workshop on pattern recognition in neuroimaging, PRNI 2011* (pp. 49–52). http://dx.doi.org/10.1109/PRNI.2011.9.

Cohen, M. X. (2015). Effects of time lag and frequency matching on phase-based connectivity. *Journal of Neuroscience Methods*, *250*, 137–146. http://dx.doi.org/10.1016/j.jneumeth.2014.09.005.

Coyle, D., Prasad, G., & McGinnity, T. M. (2005). A time-series prediction approach for feature extraction in a brain-computer interface. *IEEE Transactions on Neural Systems and Rehabilitation Engineering*, *13*(4), 461–467. http://dx.doi.org/10.1109/TNSRE.2005.857690.

Curran, E. A., & Stokes, M. J. (2003). Learning to control brain activity: A review of the production and control of EEG components for driving brain-computer interface (BCI) systems. *Brain and Cognition*, *51*(3), 326–336. http://dx.doi.org/10.1016/S0278-2626(03)00036-8, Academic Press Inc..

Daly, I., Nasuto, S. J., & Warwick, K. (2012). Brain computer interface control via functional connectivity dynamics. *Pattern Recognition*, *45*(6), 2123–2136. http://dx.doi.org/10.1016/j.patcog.2011.04.034.

Dawson, K. A. (2004). Temporal organization of the brain: Neurocognitive mechanisms and clinical implications. *Brain and Cognition*, *54*(1), 75–94. http://dx.doi.org/10.1016/S0278-2626(03)00262-8.

Decety, J. (1996). The neurophysiological basis of motor imagery. *Behavioural Brain Research*, *77*(1–2), 45–52. http://dx.doi.org/10.1016/0166-4328(95)00225-1, Elsevier B.V..

Demuru, M., & Fraschini, M. (2020). EEG Fingerprinting: Subject-specific signature based on the aperiodic component of power spectrum. *Computers in Biology and Medicine*, *120*(April), Article 103748. http://dx.doi.org/10.1016/j.compbiomed.2020.103748.

Dimitriadis, S. I., Laskaris, N. A., & Tzelepi, A. (2013). On the quantization of time-varying phase synchrony patterns into distinct functional connectivity microstates (FCμ states) in a multi-trial visual ERP paradigm. *Brain Topography*, *26*(3), 397–409. http://dx.doi.org/10.1007/s10548-013-0276-z.

Dodia, S., Edla, D. R., Bablani, A., Ramesh, D., & Kuppili, V. (2019). An efficient EEG based deceit identification test using wavelet packet transform and linear discriminant analysis. *Journal of Neuroscience Methods*, *314*, 31–40. http://dx.doi.org/10.1016/j.jneumeth.2019.01.007.

Dornhege, G., Blankertz, B., Curio, G., & Müller, K. R. (2004). Boosting bit rates in noninvasive EEG single-trial classifications by feature combination and multiclass paradigms. *IEEE Transactions on Biomedical Engineering*, *51*(6), 993–1002. http://dx.doi.org/10.1109/TBME.2004.827088.

Duckrow, R. B., & Albano, A. M. (2003). Comment on performance of different synchronization measures in real data: A case study on electroencephalographic signals. *Physical Review E - Statistical Physics, Plasmas, Fluids, and Related Interdisciplinary Topics*, *67*(6), 3. http://dx.doi.org/10.1103/PhysRevE.67.063901.

Duda, R. O., & Hart, P. E. (2000). *Pattern classification, Vol. 1* (2nd ed.). A Wiley-Interscience publication, https://www.google.com/books?hl=tr&lr=&id=Br33IRC3PkQC&oi=fnd&pg=PR3&dq=duda+pattern+classification&ots=2xEXJrg7Ft&sig=kSQjlnThzarBKogXNUWCMLjq6YU.

Emre Cek, M., Ozgoren, M., & Acar Savaci, F. (2010). Continuous time wavelet entropy of auditory evoked potentials. *Computers in Biology and Medicine*, *40*(1), 90–96. http://dx.doi.org/10.1016/j.compbiomed.2009.11.005.

Feige, B., Spiegelhalder, K., Kiemen, A., Bosch, O. G., Tebartz van Elst, L., Hennig, J., Seifritz, E., & Riemann, D. (2017). Distinctive time-lagged resting-state networks revealed by simultaneous EEG-fMRI. *NeuroImage*, *145*, 1–10. http://dx.doi.org/10.1016/j.neuroimage.2016.09.027.

Feng, J., Yin, E., Jin, J., Saab, R., Daly, I., Wang, X., Hu, D., & Cichocki, A. (2018). Towards correlation-based time window selection method for motor imagery BCIs. *Neural Networks*, *102*, 87–95. http://dx.doi.org/10.1016/j.neunet.2018.02.011.

Fingelkurts, A. A., Fingelkurts, A. A., & Kähkönen, S. (2005). Functional connectivity in the brain - is it an elusive concept?. *Neuroscience and Biobehavioral Reviews*, *28*(8), 827–836. http://dx.doi.org/10.1016/j.neubiorev.2004.10.009.

Fraschini, M., Demuru, M., Crobe, A., Marrosu, F., Stam, C. J., & Hillebrand, A. (2016). The effect of epoch length on estimated EEG functional connectivity and brain network organisation. *Journal of Neural Engineering*, *13*(3), http://dx.doi.org/10.1088/1741-2560/13/3/036015.

Friedrich, E. V. C., Scherer, R., & Neuper, C. (2012). The effect of distinct mental strategies on classification performance for brain-computer interfaces. *International Journal of Psychophysiology*, *84*(1), 86–94. http://dx.doi.org/10.1016/j.ijpsycho.2012.01.014.

Fries, P. (2005). A mechanism for cognitive dynamics: Neuronal communication through neuronal coherence. *Trends in Cognitive Sciences*, *9*(10), 474–480. http://dx.doi.org/10.1016/j.tics.2005.08.011.

Gao, Q., Duan, X., & Chen, H. (2011). Evaluation of effective connectivity of motor areas during motor imagery and execution using conditional granger causality. *NeuroImage*, *54*(2), 1280–1288. http://dx.doi.org/10.1016/j.neuroimage.2010.08.071.

Gao, Z., Li, S., Cai, Q., Dang, W., Yang, Y., Mu, C., & Hui, P. (2019). Relative wavelet entropy complex network for improving EEG-based fatigue driving classification. *IEEE Transactions on Instrumentation and Measurement*, *68*(7), 2491–2497. http://dx.doi.org/10.1109/TIM.2018.2865842.

Gao, L., Wang, J., & Chen, L. (2013). Event-related desynchronization and synchronization quantification in motor-related EEG by Kolmogorov entropy. *Journal of Neural Engineering*, *10*(3), http://dx.doi.org/10.1088/1741-2560/10/3/036023.

Göksu, H. (2018). BCI Oriented EEG analysis using log energy entropy of wavelet packets. *Biomedical Signal Processing and Control*, *44*, 101–109. http://dx.doi.org/10.1016/j.bspc.2018.04.002.

Goldberger, A. L., Amaral, L. A., Glass, L., Hausdorff, J. M., Ivanov, P. C., Mark, R. G., Mietus, J. E., Moody, G. B., Peng, C. K., & Stanley, H. E. (2000). Physiobank, physiotoolkit, and physionet: components of a new research resource for complex physiologic signals. *Circulation*, *101*(23), http://dx.doi.org/10.1161/01.cir.101.23.e215.

Golub, G. H., & Saunders, M. A. (1970). Linear least squares and quadratic programming. *Integer and Nonlinear Programming*, 229–256, https://apps.dtic.mil/docs/citations/AD0700923.

Gomez, C., Poza, J., Gomez-Pilar, J., Bachiller, A., Juan-Cruz, C., Tola-Arribas, M. A., Carreres, A., Cano, M., & Hornero, R. (2016). Analysis of spontaneous EEG activity in alzheimer's disease using cross-sample entropy and graph theory. In *Proceedings of the annual international conference of the IEEE engineering in medicine and biology society, EMBS, 2016-Octob* (pp. 2830–2833). http://dx.doi.org/10.1109/EMBC.2016.7591319.

Gómez, C., Stam, C. J., Hornero, R., Fernández, A., & Maestú, F. (2009). Disturbed beta band functional connectivity in patients with mild cognitive impairment: An MEG study. *IEEE Transactions on Biomedical Engineering*, *56*(6), 1683–1690. http://dx.doi.org/10.1109/TBME.2009.2018454.

Gonuguntla, V., Wang, Y., & Veluvolu, K. C. (2016). Event-related functional network identification: Application to EEG classification. *IEEE Journal of Selected Topics in Signal Processing*, *10*(7), 1284–1294. http://dx.doi.org/10.1109/JSTSP.2016.2602007.

Greenblatt, R. E., Pflieger, M. E., & Ossadtchi, A. E. (2012). Connectivity measures applied to human brain electrophysiological data. *Journal of Neuroscience Methods*, *207*(1), 1–16. http://dx.doi.org/10.1016/j.jneumeth.2012.02.025.

Gu, L., Yu, Z., Ma, T., Wang, H., Li, Z., & Fan, H. (2020). EEG-Based classification of lower limb motor imagery with brain network analysis. *Neuroscience*, *436*, 93–109. http://dx.doi.org/10.1016/j.neuroscience.2020.04.006.

Güdücü, C., Olcay, B. O., Schäfer, L., Aziz, M., Schriever, V. A., Özgören, M., & Hummel, T. (2019). Separating normosmic and anosmic patients based on entropy evaluation of olfactory event-related potentials. *Brain Research*, *1708*, 78–83. http://dx.doi.org/10.1016/j.brainres.2018.12.012.

Guillot, A., Desliens, S., Rouyer, C., & Rogowski, I. (2013). Motor imagery and tennis serve performance: The external focus efficacy. *Journal of Sports Science and Medicine*, *12*(2), 332–338, https://www.ncbi.nlm.nih.gov/pmc/articles/PMC3761826/.

Gürkan, G., Akan, A., & Seyhan, T. Ö. (2014). Analysis of brain connectivity changes after propofol injection by generalized partial directed coherence. *Digital Signal Processing: A Review Journal*, *25*(1), 156–163. http://dx.doi.org/10.1016/j.dsp.2013.11.011.

Halder, S., Agorastos, D., Veit, R., Hammer, E. M., Lee, S., Varkuti, B., Bogdan, M., Rosenstiel, W., Birbaumer, N., & Kübler, A. (2011). Neural mechanisms of brain-computer interface control. *NeuroImage*, *55*(4), 1779–1790. http://dx.doi.org/10.1016/j.neuroimage.2011.01.021.

Hamedi, M., Salleh, S. H., & Noor, A. M. (2016). Electroencephalographic motor imagery brain connectivity analysis for BCI: A review. *Neural Computation*, *28*(6), 999–1041. http://dx.doi.org/10.1162/NECO_a_00838, MIT Press Journals.

Hanakawa, T. (2016). Organizing motor imageries. In *Neuroscience research, Vol. 104* (pp. 56–63). Elsevier Ireland Ltd, http://dx.doi.org/10.1016/j.neures.2015.11.003.

Handiru, V. S., & Prasad, V. A. (2016). Optimized bi-objective EEG channel selection and cross-subject generalization with brain-computer interfaces. *IEEE Transactions on Human–Machine Systems*, *46*(6), 777–786. http://dx.doi.org/10.1109/THMS.2016.2573827.

Hansen, E. C. A., Battaglia, D., Spiegler, A., Deco, G., & Jirsa, V. K. (2015). Functional connectivity dynamics: Modeling the switching behavior of the resting state. *NeuroImage*, *105*, 525–535. http://dx.doi.org/10.1016/j.neuroimage.2014.11.001.

Hari, R., & Parkkonen, L. (2015). The brain timewise: How timing shapes and supports brain function. *Philosophical Transactions of the Royal Society, Series B (Biological Sciences)*, *370*(1668), http://dx.doi.org/10.1098/rstb.2014.0170.

Harrison, L., Penny, W. D., & Friston, K. (2003). Multivariate autoregressive modeling of fMRI time series. *NeuroImage*, *19*(4), 1477–1491. http://dx.doi.org/10.1016/S1053-8119(03)00160-5.

He, B., Astolfi, L., Valdes-Sosa, P. A., Marinazzo, D., Palva, S. O., Benar, C. G., Michel, C. M., & Koenig, T. (2019). Electrophysiological brain connectivity: Theory and implementation. *IEEE Transactions on Biomedical Engineering*, *66*(7), 2115–2137. http://dx.doi.org/10.1109/TBME.2019.2913928.

He, F., & Yang, Y. (2021). Nonlinear system identification of neural systems from neurophysiological signals. *Neuroscience*, http://dx.doi.org/10.1016/j.neuroscience.2020.12.001.

Herff, C., Diener, L., Angrick, M., Mugler, E., Tate, M. C., Goldrick, M. A., Krusienski, D. J., Slutzky, M. W., & Schultz, T. (2019). Generating natural, intelligible speech from brain activity in motor, premotor, and inferior frontal cortices. *Frontiers in Neuroscience*, *13*, 1267. http://dx.doi.org/10.3389/fnins.2019.01267.

Hermanto, B. R., Mengko, T. R., Indrayanto, A., & Prihatmanto, A. S. (2013). Brain signal reference concept using cross correlation based for brain computer interface. In *Proc. of 2013 3rd int. conf. on instrumentation, communications, information technol., and biomedical engineering: science and technol. for improvement of health, safety, and environ., ICICI-BME 2013* (pp. 388–391). http://dx.doi.org/10.1109/ICICI-BME.2013.6698531.

Hétu, S., Grégoire, M., Saimpont, A., Coll, M. P., Eugène, F., Michon, P. E., & Jackson, P. L. (2013). The neural network of motor imagery: An ALE meta-analysis. *Neuroscience and Biobehavioral Reviews*, *37*(5), 930–949. http://dx.doi.org/10.1016/j.neubiorev.2013.03.017, Pergamon.

Higashi, H., & Tanaka, T. (2013). Simultaneous design of FIR filter banks and spatial patterns for EEG signal classification. *IEEE Transactions on Biomedical Engineering*, *60*(4), 1100–1110. http://dx.doi.org/10.1109/TBME.2012.2215960.

Hipp, J. F., Hawellek, D. J., Corbetta, M., Siegel, M., & Engel, A. K. (2012). Large-scale cortical correlation structure of spontaneous oscillatory activity. *Nature Neuroscience*, *15*(6), 884–890. http://dx.doi.org/10.1038/nn.3101.

Höller, Y., Bergmann, J., Kronbichler, M., Crone, J. S., Schmid, E. V., Thomschewski, A., Butz, K., Schütze, V., Höller, P., & Trinka, E. (2013). Real movement vs. motor imagery in healthy subjects. *International Journal of Psychophysiology*, *87*(1), 35–41. http://dx.doi.org/10.1016/j.ijpsycho.2012.10.015.

Hramov, A. E., Maksimenko, V., Koronovskii, A., Runnova, A. E., Zhuravlev, M., Pisarchik, A. N., & Kurths, J. (2019). Percept-related EEG classification using machine learning approach and features of functional brain connectivity. *Chaos*, *29*(9), http://dx.doi.org/10.1063/1.5113844.

Hsu, W. Y., Lin, C. C., Ju, M. S., & Sun, Y. N. (2007). Wavelet-based fractal features with active segment selection: Application to single-trial EEG data. *Journal of Neuroscience Methods*, *163*(1), 145–160. http://dx.doi.org/10.1016/j.jneumeth.2007.02.004.

Hsu, W. Y., & Sun, Y. N. (2009). EEG-Based motor imagery analysis using weighted wavelet transform features. *Journal of Neuroscience Methods*, *176*(2), 310–318. http://dx.doi.org/10.1016/j.jneumeth.2008.09.014.

Hutchison, R. M., Womelsdorf, T., Allen, E. A., Bandettini, P. A., Calhoun, V. D., Corbetta, M., Della Penna, S., Duyn, J. H., Glover, G. H., Gonzalez-Castillo, J., Handwerker, D. A., Keilholz, S., Kiviniemi, V., Leopold, D. A., Pasquale, F. de., Sporns, O., Walter, M., & Chang, C. (2013). Dynamic functional connectivity: Promise, issues, and interpretations. *NeuroImage*, *80*, 360–378. http://dx.doi.org/10.1016/j.neuroimage.2013.05.079.

Hyvärinen, A., & Oja, E. (2000). Independent component analysis: Algorithms and applications. *Neural Networks*, *13*(4–5), 411–430. http://dx.doi.org/10.1016/S0893-6080(00)00026-5.

Ibrahim Al-Omari, A. (2014). Estimation of entropy using random sampling. *Journal of Computational and Applied Mathematics*, *261*, 95–102. http://dx.doi.org/10.1016/j.cam.2013.10.047.

Ince, N. F., Goksu, F., Tewfik, A. H., & Arica, S. (2009). Adapting subject specific motor imagery EEG patterns in space–time-frequency for a brain computer interface. *Biomedical Signal Processing and Control*, *4*(3), 236–246. http://dx.doi.org/10.1016/j.bspc.2009.03.005.

Ince, N. F., Tewfik, A. H., & Arica, S. (2007). Extraction subject-specific motor imagery time-frequency patterns for single trial EEG classification. *Computers in Biology and Medicine*, *37*(4), 499–508. http://dx.doi.org/10.1016/j.compbiomed.2006.08.014.

Izumi, S. I., Findley, T. W., Ikai, T., Andrews, J., Daum, M., & Chino, N. (1995). Facilitatory effect of thinking about movement on motor-evoked potentials to transcranial magnetic stimulation of the brain. *American Journal of Physical Medicine and Rehabilitation*, *74*(3), 207–213. http://dx.doi.org/10.1097/00002060-199505000-00005.

Jeong, J., Gore, J. C., & Peterson, B. S. (2001). Mutual information analysis of the EEG in patients with alzheimer's disease. *Clinical Neurophysiology*, *112*(5), 827–835. http://dx.doi.org/10.1016/S1388-2457(01)00513-2.

Jian, W., Chen, M., & McFarland, . D. J. (2017). EEG Based zero-phase phase-locking value (PLV) and effects of spatial filtering during actual movement. *Brain Research Bulletin*, *130*, 156–164. http://dx.doi.org/10.1016/j.brainresbull.2017.01.023.

Jin, S. H., Kwon, Y. J., Jeong, J. S., Kwon, S. W., & Shin, D. H. (2006). Increased information transmission during scientific hypothesis generation: Mutual information analysis of multichannel EEG. *International Journal of Psychophysiology*, *62*(2), 337–344. http://dx.doi.org/10.1016/j.ijpsycho.2006.06.003.

Jin, S. H., Lin, P., & Hallett, M. (2010). Linear and nonlinear information flow based on time-delayed mutual information method and its application to corticomuscular interaction. *Clinical Neurophysiology*, *121*(3), 392–401. http://dx.doi.org/10.1016/j.clinph.2009.09.033.

Jin, S. H., Lin, P., & Hallett, M. (2012). Reorganization of brain functional small-world networks during finger movements. *Human Brain Mapping*, *33*(4), 861–872. http://dx.doi.org/10.1002/hbm.21253.

Jolliffe, I. T. (1986). *Principal component analysis*, *Principal components in regression analysis* (pp. 129–155). Springer, http://dx.doi.org/10.1007/978-1-4757-1904-8_8.

Karamzadeh, N., Medvedev, A., Azari, A., Gandjbakhche, A., & Najafizadeh, L. (2013). Capturing dynamic patterns of task-based functional connectivity with EEG. *NeuroImage*, *66*, 311–317. http://dx.doi.org/10.1016/j.neuroimage.2012.10.032.

Kasess, C. H., Windischberger, C., Cunnington, R., Lanzenberger, R., Pezawas, L., & Moser, E. (2008). The suppressive influence of SMA on M1 in motor imagery revealed by fMRI and dynamic causal modeling. *NeuroImage*, *40*(2), 828–837. http://dx.doi.org/10.1016/j.neuroimage.2007.11.040.

Kee, C. Y., Ponnambalam, S. G., & Loo, C. K. (2017). Binary and multi-class motor imagery using renyi entropy for feature extraction. *Neural Computing and Applications*, *28*(8), 2051–2062. http://dx.doi.org/10.1007/s00521-016-2178-y.

Kelso, J. A. S., Dumas, G., & Tognoli, E. (2013). Outline of a general theory of behavior and brain coordination. *Neural Networks*, *37*, 120–131. http://dx.doi.org/10.1016/j.neunet.2012.09.003.

Kevric, J., & Subasi, A. (2017). Comparison of signal decomposition methods in classification of EEG signals for motor-imagery BCI system. *Biomedical Signal Processing and Control*, *31*, 398–406. http://dx.doi.org/10.1016/j.bspc.2016.09.007.

Kilintari, M., Narayana, S., Babajani-Feremi, A., Rezaie, R., & Papanicolaou, A. C. (2016). Brain activation profiles during kinesthetic and visual imagery: An fMRI study. *Brain Research*, *1646*, 249–261. http://dx.doi.org/10.1016/j.brainres.2016.06.009.

Kim, Y., Ryu, J., Kim, K. K., Took, C. C., Mandic, D. P., & Park, C. (2016). Motor imagery classification using mu and beta rhythms of EEG with strong uncorrelating transform based complex common spatial patterns. *Computational Intelligence and Neuroscience*, *2016*(1), http://dx.doi.org/10.1155/2016/1489692.

Kirschner, A., Kam, J. W. Y., Handy, T. C., & Ward, L. M. (2012). Differential synchronization in default and task-specific networks of the human brain. *Frontiers in Human Neuroscience*, *6*(MAY 2012), 1–10. http://dx.doi.org/10.3389/fnhum.2012.00139.

Korostenskaja, M., Kapeller, C., Lee, K. H., Guger, C., Baumgartner, J., & Castillo, E. M. (2017). Characterization of cortical motor function and imagery-related cortical activity: Potential application for prehabilitation. In *2017 IEEE international conference on systems, man, and cybernetics, SMC 2017, 2017-Janua* (pp. 3014–3019). http://dx.doi.org/10.1109/SMC.2017.8123087.

Kraeutner, S., Gionfriddo, A., Bardouille, T., & Boe, S. (2014). Motor imagery-based brain activity parallels that of motor execution: Evidence from magnetic source imaging of cortical oscillations. *Brain Research*, *1588*, 81–91. http://dx.doi.org/10.1016/j.brainres.2014.09.001.

Kraskov, A., Stögbauer, H., & Grassberger, P. (2004). Estimating mutual information. *Physical Review E - Statistical Physics, Plasmas, Fluids, and Related Interdisciplinary Topics*, *69*(6), 16. http://dx.doi.org/10.1103/PhysRevE.69.066138.

Ktonas, P. Y., & Mallart, R. (1991). Estimation of time delay between EEG signals for epileptic focus localization: statistical error considerations. *Electroencephalography and Clinical Neurophysiology*, *78*(2), 105–110. http://dx.doi.org/10.1016/0013-4694(91)90109.

Kumar, S., Sharma, A., & Tsunoda, T. (2017). An improved discriminative filter bank selection approach for motor imagery EEG signal classification using mutual information. *BMC Bioinformatics*, 18. http://dx.doi.org/10.1186/s12859-017-1964-6.

Kuruoğlu, E. E. (2002). Nonlinear least lp-norm filters for nonlinear autoregressive α-stable processes. *Digital Signal Processing: A Review Journal*, *12*(1), 119–142. http://dx.doi.org/10.1006/dspr.2001.0416.

Lachaux, J. P., Rodriguez, E., Martinerie, J., & Varela, F. J. (1999). Measuring phase synchrony in brain signals. *Human Brain Mapping*, *8*(4), 194–208. http://dx.doi.org/10.1002/(SICI)1097-0193(1999)8:4<194::AID-HBM4>3.0.CO;2-C.

Lafleur, K., Cassady, K., Doud, A., Shades, K., Rogin, E., & He, B. (2013). Quadcopter control in three-dimensional space using a noninvasive motor imagery-based brain-computer interface. *Journal of Neural Engineering*, *10*(4), http://dx.doi.org/10.1088/1741-2560/10/4/046003.

Lemm, S., Blankertz, B., Curio, G., & Müller, K. R. (2005). Spatio-spectral filters for improving the classification of single trial EEG. *IEEE Transactions on Biomedical Engineering*, *52*(9), 1541–1548. http://dx.doi.org/10.1109/TBME.2005.851521.

Li, G., Jiang, D., Zhou, Y., Jiang, G., Kong, J., & Manogaran, G. (2019). Human lesion detection method based on image information and brain signal. *IEEE Access*, *7*, 11533–11542. http://dx.doi.org/10.1109/ACCESS.2019.2891749.

Li, Y., Lei, M., Cui, W., Guo, Y., & Wei, H. L. (2019). A parametric time-frequency conditional granger causality method using ultra-regularized orthogonal least squares and multiwavelets for dynamic connectivity analysis in EEGs. *IEEE Transactions on Biomedical Engineering*, *66*(12), 3509–3525. http://dx.doi.org/10.1109/TBME.2019.2906688.

Li, G., Li, J., Ju, Z., Sun, Y., & Kong, J. (2019). A novel feature extraction method for machine learning based on surface electromyography from healthy brain. *Neural Computing and Applications*, *31*(12), 9013–9022. http://dx.doi.org/10.1007/s00521-019-04147-3.

Li, J., Wang, Y., Zhang, L., Cichocki, A., & Jung, T. P. (2016). Decoding EEG in cognitive tasks with time-frequency and connectivity masks. *IEEE Transactions on Cognitive and Developmental Systems*, *8*(4), 298–308. http://dx.doi.org/10.1109/TCDS.2016.2555952.

Lin, A., Liu, K. K. L., Bartsch, R. P., & Ivanov, P. C. (2020). Dynamic network interactions among distinct brain rhythms as a hallmark of physiologic state and function. *Communications Biology*, *3*(1), 197. http://dx.doi.org/10.1038/s42003-020-0878-4.

Liu, W., Pokharel, P. P., & Principe, J. C. (2007). Correntropy: Properties and applications in non-Gaussian signal processing. *IEEE Transactions on Signal Processing*, *55*(11), 5286–5298. http://dx.doi.org/10.1109/TSP.2007.896065.

Llanos, C., Rodriguez, M., Rodriguez-Sabate, C., Morales, I., & Sabate, M. (2013). Mu-rhythm changes during the planning of motor and motor imagery actions. *Neuropsychologia*, *51*(6), 1019–1026. http://dx.doi.org/10.1016/j.neuropsychologia.2013.02.008.

Lotte, F. (2008). *Study of electroencephalographic signal processing and classification techniques towards the use of brain-computer interfaces in virtual reality applications* (Thesis), http://tel.archives-ouvertes.fr/tel-00356346/en/.

Lotte, F., & Guan, C. (2011). Regularizing common spatial patterns to improve BCI designs: Unified theory and new algorithms. *IEEE Transactions on Biomedical Engineering*, *58*(2), 355–362. http://dx.doi.org/10.1109/TBME.2010.2082539.

Lu, C. F., Teng, S., Hung, C. I., Tseng, P. J., Lin, L. T., Lee, P. L., & Wu (2011). Reorganization of functional connectivity during the motor task using EEG time-frequency cross mutual information analysis. *Clinical Neurophysiology*, *122*(8), 1569–1579. http://dx.doi.org/10.1016/j.clinph.2011.01.050.

Lu, R. R., Zheng, M. X., Li, J., Gao, T. H., Hua, X. Y., Liu, G., Huang, S. H., Xu, J. G., & Wu, Y. (2020). Motor imagery based brain-computer interface control of continuous passive motion for wrist extension recovery in chronic stroke patients. *Neuroscience Letters*, 718. http://dx.doi.org/10.1016/j.neulet.2019.134727.

Ludwig, K. A., Miriani, R. M., Langhals, N. B., Joseph, M. D., Anderson, D. J., & Kipke, D. R. (2009). Using a common average reference to improve cortical neuron recordings from microelectrode arrays. *Journal of Neurophysiology*, *101*(3), 1679–1689. http://dx.doi.org/10.1152/jn.90989.2008.

Maars, N. J. I., & Lopes Da Silva, F. H. (1983). Propagation of seizure activity in kindled dogs. *Electroencephalography and Clinical Neurophysiology*, *56*(2), 194–209. http://dx.doi.org/10.1016/0013-4694(83)90074-3.

Makarov, V. V., Zhuravlev, M. O., Runnova, A. E., Protasov, P., Maksimenko, V. A., Frolov, N. S., Pisarchik, A. N., & Hramov, A. E. (2018). Betweenness centrality in multiplex brain network during mental task evaluation. *Physical Review E*, *98*(6), 1–9. http://dx.doi.org/10.1103/PhysRevE.98.062413.

Marinazzo, D., Liao, W., Chen, H., & Stramaglia, S. (2011). Nonlinear connectivity by granger causality. *NeuroImage*, *58*(2), 330–338. http://dx.doi.org/10.1016/j.neuroimage.2010.01.099.

McFarland, D. J., McCane, L. M., David, S. V., & Wolpaw, J. R. (1997). Spatial filter selection for EEG-based communication. *Electroencephalography and Clinical Neurophysiology*, *103*(3), 386–394. http://dx.doi.org/10.1016/S0013-4694(97)00022-2.

McFarland, D. J., & Wolpaw, J. R. (2008). Sensorimotor rhythm-based brain-computer interface (BCI): Model order selection for autoregressive spectral analysis. *Journal of Neural Engineering*, *5*(2), 155–162. http://dx.doi.org/10.1088/1741-2560/5/2/006.

Melia, U., Guaita, M., Vallverdú, M., Embid, C., Vilaseca, I., Salamero, M., & Santamaria, J. (2015). Mutual informationmeasuresapplied to EEG signals for sleepiness characterization. *Medical Engineering & Physics*, *37*(3), 297–308. http://dx.doi.org/10.1016/j.medengphy.2015.01.002.

Melia, U., Guaita, M., Vallverdú, M., Montserrat, J. M., Vilaseca, I., Salamero, M., Gaig, C., Caminal, P., & Santamaria, J. (2014). Correntropy measures to detect daytime sleepiness from EEG signals. *Physiological Measurement*, *35*(10), 2067–2083. http://dx.doi.org/10.1088/0967-3334/35/10/2067.

Menicucci, D., Di Gruttola, F., Cesari, V., Gemignani, A., Manzoni, D., & Sebastiani, L. (2020). Task-independent electrophysiological correlates of motor imagery ability from kinaesthetic and visual perspectives. *Neuroscience*, *443*, 176–187. http://dx.doi.org/10.1016/j.neuroscience.2020.07.038.

Mijalkov, M., Pereira, J. B., & Volpe, G. (2020). Delayed correlations improve the reconstruction of the brain connectome. *PLoS One*, *15*(2), Article e0228334. http://dx.doi.org/10.1371/journal.pone.0228334.

Milton, J., Solodkin, A., Hluštík, P., & Small, S. L. (2007). The mind of expert motor performance is cool and focused. *NeuroImage*, *35*(2), 804–813. http://dx.doi.org/10.1016/j.neuroimage.2007.01.003.

Mišić, B., & Sporns, O. (2016). From regions to connections and networks: New bridges between brain and behavior. In *Current opinion in neurobiology, Vol. 40* (pp. 1–7). http://dx.doi.org/10.1016/j.conb.2016.05.003.

Mitra, A., Snyder, A. Z., Blazey, T., & Raichle, M. E. (2015). Lag threads organize the brain's intrinsic activity. *Proceedings of the National Academy of Sciences of the United States of America*, *112*(17), E2235–E2244. http://dx.doi.org/10.1073/pnas.1503960112.

Müller-Putz, G. R., Scherer, R., Brunner, C., Leeb, R., & Pfurtscheller, G. (2007). Better than random: a closer look on BCI results. In *2007 1st cost neuromath workgroup meeting, Rome, Italy, Vol. 10(1)* (pp. 95–96). http://infoscience.epfl.ch/record/164768.

Munzert, J., Lorey, B., & Zentgraf, K. (2009). Cognitive motor processes: The role of motor imagery in the study of motor representations. *Brain Research Reviews*, *60*(2), 306–326. http://dx.doi.org/10.1016/j.brainresrev.2008.12.024.

Na, S. H., Jin, S. H., Kim, S. Y., & Ham, B. J. (2002). EEG In schizophrenic patients: Mutual information analysis. *Clinical Neurophysiology*, *113*(12), 1954–1960. http://dx.doi.org/10.1016/S1388-2457(02)00197-9.

Neuper, C., Scherer, R., Reiner, M., & Pfurtscheller, G. (2005). Imagery of motor actions: Differential effects of kinesthetic and visual-motor mode of imagery in single-trial EEG. *Cognitive Brain Research*, *25*(3), 668–677. http://dx.doi.org/10.1016/j.cogbrainres.2005.08.014.

Neuper, C., Scherer, R., Wriessnegger, S., & Pfurtscheller, G. (2009). Motor imagery and action observation: Modulation of sensorimotor brain rhythms during mental control of a brain-computer interface. *Clinical Neurophysiology*, *120*(2), 239–247. http://dx.doi.org/10.1016/j.clinph.2008.11.015.

Nguyen-Ky, T., Wen, P., Li, Y., & Malan, M. (2012). Measuring the hypnotic depth of anaesthesia based on the EEG signal using combined wavelet transform, eigenvector and normalisation techniques. *Computers in Biology and Medicine*, *42*(6), 680–691. http://dx.doi.org/10.1016/j.compbiomed.2012.03.004.

Nolte, G., Bai, O., Wheaton, L., Mari, Z., Vorbach, S., & Hallett, M. (2004). Identifying true brain interaction from EEG data using the imaginary part of coherency. *Clinical Neurophysiology*, *115*(10), 2292–2307. http://dx.doi.org/10.1016/j.clinph.2004.04.029.

Olcay, Bilal Orkan, Karacali, B., Ozgoren, M., & Guducu, C. (2017). Entropik Kümeleme kullanilarak beyin aktivitesi karakteriz asyonu. In *2017 25th signal processing and communications applications conference, SIU 2017* (pp. 1–4). http://dx.doi.org/10.1109/SIU.2017.7960503.

Olcay, B. Orkan, & Karaçalı, B. (2019). Evaluation of synchronization measures for capturing the lagged synchronization between EEG channels: A cognitive task recognition approach. *Computers in Biology and Medicine*, *114*, Article 103441. http://dx.doi.org/10.1016/j.compbiomed.2019.103441.

Olejarczyk, E., Marzetti, L., Pizzella, V., & Zappasodi, F. (2017). Comparison of connectivity analyses for resting state EEG data. *Journal of Neural Engineering*, *14*(3), http://dx.doi.org/10.1088/1741-2552/aa6401.

Palmigiano, A., Geisel, T., Wolf, F., & Battaglia, D. (2017). Flexible information routing by transient synchrony. *Nature Neuroscience*, *20*(7), 1014–1022. http://dx.doi.org/10.1038/nn.4569.

Pani, S. M., Ciuffi, M., Demuru, M., La Cava, S. M., Bazzano, G., D'Aloja, E., & Fraschini, M. (2020). Subject, session and task effects on power, connectivity and network centrality: A source-based EEG study. *Biomedical Signal Processing and Control*, *59*, Article 101891. http://dx.doi.org/10.1016/j.bspc.2020.101891.

Park, Chang hyun, Chang, W. H., Lee, M., Kwon, G. H., Kim, L., Kim, S. T., & Kim, Y. H. (2015). Which motor cortical region best predicts imagined movement?. *NeuroImage*, *113*, 101–110. http://dx.doi.org/10.1016/j.neuroimage.2015.03.033.

Park, S. H., Lee, D., & Lee, S. G. (2018). Filter bank regularized common spatial pattern ensemble for small sample motor imagery classification. *IEEE Transactions on Neural Systems and Rehabilitation Engineering*, *26*(2), 498–505. http://dx.doi.org/10.1109/TNSRE.2017.2757519.

Park, Cheolsoo, Looney, D., Ur Rehman, N., Ahrabian, A., & Mandic, D. P. (2013). Classification of motor imagery BCI using multivariate empirical mode decomposition. *IEEE Transactions on Neural Systems and Rehabilitation Engineering*, *21*(1), 10–22. http://dx.doi.org/10.1109/TNSRE.2012.2229296.

Park, Cheolsoo, Took, C. C., & Mandic, D. P. (2014). Augmented complex common spatial patterns for classification of noncircular EEG from motor imagery tasks. *IEEE Transactions on Neural Systems and Rehabilitation Engineering*, *22*(1), 1–10. http://dx.doi.org/10.1109/TNSRE.2013.2294903.

Patel, M., & Joshi, B. (2013). Decoding synchronized oscillations within the brain: Phase-delayed inhibition provides a robust mechanism for creating a sharp synchrony filter. *Journal of Theoretical Biology*, *334*, 13–25. http://dx.doi.org/10.1016/j.jtbi.2013.05.022.

Peng, H., Xia, C., Wang, Z., Zhu, J., Zhang, X., Sun, S., Li, J., Huo, X., & Li, X. (2019). Multivariate pattern analysis of EEG-based functional connectivity: A study on the identification of depression. *IEEE Access*, *7*, 92630–92641. http://dx.doi.org/10.1109/ACCESS.2019.2927121.

Pereda, E., Quiroga, R. Q., & Bhattacharya, J. (2005). Nonlinear multivariate analysis of neurophysiological signals. *Progress in Neurobiology*, *77*(1–2), 1–37. http://dx.doi.org/10.1016/j.pneurobio.2005.10.003.

Pfurtscheller, G., & Berghold, A. (1989). Patterns of cortical activation during planning of voluntary movement. *Electroencephalography and Clinical Neurophysiology*, *72*(3), 250–258. http://dx.doi.org/10.1016/0013-4694(89)90250-2.

Pfurtscheller, Gert, Leeb, R., Keinrath, C., Friedman, D., Neuper, C., Guger, C., & Slater, M. (2006). Walking from thought. *Brain Research*, *1071*(1), 145–152. http://dx.doi.org/10.1016/j.brainres.2005.11.083.

Pfurtscheller, Gert, & Neuper, C. (1997). Motor imagery activates primary sensorimotor area in humans. *Neuroscience Letters*, *239*(2–3), 65–68. http://dx.doi.org/10.1016/S0304-3940(97)00889-6.

Pfurtscheller, G., Neuper, C., Guger, C., Harkam, W., Ramoser, H., Schlögl, A., Obermaier, B., & Pregenzer, M. (2000). Current trends in graz brain-computer interface (BCI) research. *IEEE Transactions on Rehabilitation Engineering*, *8*(2), 216–219. http://dx.doi.org/10.1109/86.847821.

Pfurtscheller, G., Scherer, R., Müller-Putz, G. R., & Lopes Da Silva, F. H. (2008). Short-lived brain state after cued motor imagery in naive subjects. *European Journal of Neuroscience*, *28*(7), 1419–1426. http://dx.doi.org/10.1111/j.1460-9568.2008.06441.x.

Porro, C. A., Cettolo, V., Francescato, M. P., & Baraldi, P. (2000). Ipsilateral involvement of primary motor cortex during motor imagery. *European Journal of Neuroscience*, *12*(8), 3059–3063. http://dx.doi.org/10.1046/j.1460-9568.2000.00182.x.

Principe, J. C. (2010). Information theoretic learning: Rényi entropy and kernel perspectives. (p. 515).

Qian, Y., Zhao, Y., Liu, F., Huang, X., Zhang, Z., & Mi, Y. (2013). Effects of time delay and coupling strength on synchronization transitions in excitable homogeneous random network. *Communications in Nonlinear Science and Numerical Simulation*, *18*(12), 3509–3516. http://dx.doi.org/10.1016/j.cnsns.2013.05.008.

Rabinovich, M. I., & Muezzinoglu, M. K. (2010). Nonlinear dynamics of the brain: emotion and cognition. *Physics-Uspekhi*, *53*(4), 357–372. http://dx.doi.org/10.3367/ufne.0180.201004b.0371.

Ramoser, H., Müller-Gerking, J., & Pfurtscheller, G. (2000). Optimal spatial filtering of single trial EEG during imagined hand movement. *IEEE Transactions on Rehabilitation Engineering*, *8*(4), 441–446. http://dx.doi.org/10.1109/86.895946.

Rao, M., Seth, S., Xu, J., Chen, Y., Tagare, H., & Príncipe, J. C. (2011). A test of independence based on a generalized correlation function. *Signal Processing*, *91*(1), 15–27. http://dx.doi.org/10.1016/j.sigpro.2010.06.002.

Rathee, D., Raza, H., Prasad, G., & Cecotti, H. (2017). Current source density estimation enhances the performance of motor-imagery-related brain–computer interface. *IEEE Transactions on Neural Systems and Rehabilitation Engineering*, *25*(12), 2461–2471. http://dx.doi.org/10.1109/TNSRE.2017.2726779.

Ren, S., Li, J., Taya, F., DeSouza, J., Thakor, N. V., & Bezerianos, A. (2017). Dynamic functional segregation and integration in human brain network during complex tasks. *IEEE Transactions on Neural Systems and Rehabilitation Engineering*, *25*(6), 547–556. http://dx.doi.org/10.1109/TNSRE.2016.2597961.

Rocca, D. La, Campisi, P., Vegso, B., Cserti, P., Kozmann, G., Babiloni, F., & De Vico Fallani, F. (2014). Human brain distinctiveness based on EEG spectral coherence connectivity. *IEEE Transactions on Biomedical Engineering*, *61*(9), 2406–2412. http://dx.doi.org/10.1109/TBME.2014.2317881.

Rodu, J., Klein, N., Brincat, S. L., Miller, E. K., & Kass, R. E. (2018). Detecting multivariate cross-correlation between brain regions. *Journal of Neurophysiology*, *120*(4), 1962–1972. http://dx.doi.org/10.1152/jn.00869.2017.

Roelfsema, P. R., Engel, A. K., König, P., & Singer, W. (1997). Visuomotor integration is associated with zero time-lag synchronization among cortical areas. *Nature*, *385*(6612), 157–161. http://dx.doi.org/10.1038/385157a0.

Rosso, Osvaldo A., Blanco, S., Yordanova, J., Kolev, V., Figliola, A., Schürmann, M., & Ba ar, E. (2001). Wavelet entropy: A new tool for analysis of short duration brain electrical signals. *Journal of Neuroscience Methods*, *105*(1), 65–75. http://dx.doi.org/10.1016/S0165-0270(00)00356-3.

Rosso, O. A., Martin, M. T., Figliola, A., Keller, K., & Plastino, A. (2006). EEG Analysis using wavelet-based information tools. *Journal of Neuroscience Methods*, *153*(2), 163–182. http://dx.doi.org/10.1016/j.jneumeth.2005.10.009.

Rubinov, M., & Sporns, O. (2010). Complex network measures of brain connectivity: Uses and interpretations. *NeuroImage*, *52*(3), 1059–1069. http://dx.doi.org/10.1016/j.neuroimage.2009.10.003.

Sakkalis, V. (2011). Review of advanced techniques for the estimation of brain connectivity measured with EEG/meg. *Computers in Biology and Medicine*, *41*(12), 1110–1117. http://dx.doi.org/10.1016/j.compbiomed.2011.06.020.

Salyers, J. B., Dong, Y., & Gai, Y. (2019). Continuous wavelet transform for decoding finger movements from single-channel EEG. *IEEE Transactions on Biomedical Engineering*, *66*(6), 1588–1597. http://dx.doi.org/10.1109/TBME.2018.2876068.

Samdin, S. B., Ting, C. M., Ombao, H., & Salleh, S. H. (2017). A unified estimation framework for state-related changes in effective brain connectivity. *IEEE Transactions on Biomedical Engineering*, *64*(4), 844–858. http://dx.doi.org/10.1109/TBME.2016.2580738.

Santamaria, L., & James, C. (2019). On the existence of phase-synchronised states during motor imagery tasks. *Biomedical Signal Processing and Control*, *54*, Article 101630. http://dx.doi.org/10.1016/j.bspc.2019.101630.

Santamaría, I., Pokharel, P. P., & Principe, J. C. (2006). Generalized correlation function: Definition, properties, and application to blind equalization. *IEEE Transactions on Signal Processing*, *54*(6 I), 2187–2197. http://dx.doi.org/10.1109/TSP.2006.872524.

Sargolzaei, S., Cabrerizo, M., Goryawala, M., Eddin, A. S., & Adjouadi, M. (2015). Scalp EEG brain functional connectivity networks in pediatric epilepsy. *Computers in Biology and Medicine*, *56*, 158–166. http://dx.doi.org/10.1016/j.compbiomed.2014.10.018.

Sarmukadam, K., Bitsika, V., Sharpley, C. F., McMillan, M. M. E., & Agnew, L. L. (2020). Comparing different EEG connectivity methods in young males with ASD. *Behavioural Brain Research*, 383. http://dx.doi.org/10.1016/j.bbr.2020.112482.

Schack, B., Weiss, S., & Rappelsberger, P. (2003). Cerebral information transfer during word processing: Where and when does it occur and how fast is it?. *Human Brain Mapping*, *19*(1), 18–36. http://dx.doi.org/10.1002/hbm.10104.

Schalk, G., McFarland, . D. J., Hinterberger, T., Birbaumer, N., & Wolpaw, J. R. (2004). BCI2000: A general-purpose brain-computer interface (BCI) system. *IEEE Transactions on Biomedical Engineering*, *51*(6), 1034–1043. http://dx.doi.org/10.1109/TBME.2004.827072.

Schlögl, A. (2000). *The electroencephalogram and the adaptive autoregressive model: theory and applications*. Shaker.

Schreiber, T. (2000). Measuring information transfer. *Physical Review Letters*, *85*(2), 461–464. http://dx.doi.org/10.1103/PhysRevLett.85.461.

Sideridis, G., Simos, P., Papanicolaou, A., & Fletcher, J. (2014). Using structural equation modeling to assess functional connectivity in the brain: Power and sample size considerations. *Educational and Psychological Measurement*, *74*(5), 733–758. http://dx.doi.org/10.1177/0013164414525397.

Skidmore, F., Korenkevych, D., Liu, Y., He, G., Bullmore, E., & Pardalos, P. M. (2011). Connectivity brain networks based on wavelet correlation analysis in parkinson fMRI data. *Neuroscience Letters*, *499*(1), 47–51. http://dx.doi.org/10.1016/j.neulet.2011.05.030.

Solomon, J. P., Kraeutner, S. N., Bardouille, T., & Boe, S. G. (2019). Probing the temporal dynamics of movement inhibition in motor imagery. *Brain Research*, *1720*(June), Article 146310. http://dx.doi.org/10.1016/j.brainres.2019.146310.

Song, L., & Epps, J. (2007). Classifying EEG for brain-computer interface: Learning optimal filters for dynamical system features. *Computational Intelligence and Neuroscience*, (2007), http://dx.doi.org/10.1155/2007/57180.

Spiegler, A., Graimann, B., & Pfurtscheller, G. (2004). Phase coupling between different motor areas during tongue-movement imagery. *Neuroscience Letters*, *369*(1), 50–54. http://dx.doi.org/10.1016/j.neulet.2004.07.054.

Sporns, Olaf, Chialvo, D. R., Kaiser, M., & Hilgetag, C. C. (2004). Organization, development and function of complex brain networks. *Trends in Cognitive Sciences*, *8*(9), 418–425. http://dx.doi.org/10.1016/j.tics.2004.07.008.

Sporns, O., Tononi, G., & Edelman, G. M. (2000). Connectivity and complexity: The relationship between neuroanatomy and brain dynamics. *Neural Networks*, *13*(8–9), 909–922. http://dx.doi.org/10.1016/S0893-6080(00)00053-8, Elsevier Science Ltd.

Stam, C. J. (2005). Nonlinear dynamical analysis of EEG and MEG: Review of an emerging field. *Clinical Neurophysiology*, *116*(10), 2266–2301. http://dx.doi.org/10.1016/j.clinph.2005.06.011, Elsevier.

Stam, Cornelis J., Breakspear, M., Van Cappellen van Walsum, A. M., & Van Dijk, B. W. (2003). Nonlinear synchronization in EEG and whole-head MEG recordings of healthy subjects. *Human Brain Mapping*, *19*(2), 63–78. http://dx.doi.org/10.1002/hbm.10106.

Stam, Cornelis J., Nolte, G., & Daffertshofer, A. (2007). Phase lag index: Assessment of functional connectivity from multi channel EEG and MEG with diminished bias from common sources. *Human Brain Mapping*, *28*(11), 1178–1193. http://dx.doi.org/10.1002/hbm.20346.

Stam, C. J., & van Straaten, E. C. W. (2012). The organization of physiological brain networks. *Clinical Neurophysiology*, *123*(6), 1067–1087. http://dx.doi.org/10.1016/j.clinph.2012.01.011.

Stam, C. J., & Van Dijk, B. W. (2002). Synchronization likelihood: An unbiased measure of generalized synchronization in multivariate data sets. *Physica D: Nonlinear Phenomena*, *163*(3–4), 236–251. http://dx.doi.org/10.1016/S0167-2789(01)00386-4.

Sun, Y., Xu, C., Li, G., Xu, W., Kong, J., Jiang, D., Tao, B., & Chen, D. (2020). Intelligent human computer interaction based on non redundant EMG signal. *AlexandRia Engineering Journal*, *59*(3), 1149–1157. http://dx.doi.org/10.1016/j.aej.2020.01.015.

Tass, P., Rosenblum, M. G., Weule, J., Kurths, J., Pikovsky, A., Volkmann, J., Schnitzler, A., & Freund, H. J. (1998). Detection of n:m phase locking from noisy data: Application to magnetoencephalography. *Physical Review Letters*, *81*(15), 3291–3294. http://dx.doi.org/10.1103/PhysRevLett.81.3291, World Scientific.

Telesford, Q. K., Simpson, S. L., Burdette, J. H., Hayasaka, S., & Laurienti, P. J. (2011). The brain as a complex system: Using network science as a tool for understanding the brain. *Brain Connectivity*, *1*(4), 295–308. http://dx.doi.org/10.1089/brain.2011.0055.

Tirsch, W. S., Stude, P., Scherb, H., & Keidel, M. (2004). Temporal order of nonlinear dynamics in human brain. *Brain Research Reviews*, *45*(2), 79–95. http://dx.doi.org/10.1016/j.brainresrev.2004.01.002.

Tognoli, E., & Kelso, J. A. S. (2009). Brain coordination dynamics: True and false faces of phase synchrony and metastability. *Progress in Neurobiology*, *87*(1), 31–40. http://dx.doi.org/10.1016/j.pneurobio.2008.09.014.

Tolić, M., & Jović, F. (2013). Classification of wavelet transformed EEG signals with neural network for imagined mental and motor tasks. *Kinesiology*, *45*(1), 130–138.

Tsuchimoto, S., Shibusawa, S., Iwama, S., Hayashi, M., Okuyama, K., Mizuguchi, N., Kato, K., & Ushiba, J. (2021). Use of common average reference and large-Laplacian spatial-filters enhances EEG signal-to-noise ratios in intrinsic sensorimotor activity. *Journal of Neuroscience Methods*, *353*(2020), Article 109089. http://dx.doi.org/10.1016/j.jneumeth.2021.109089.

Tzovara, A., Murray, M. M., Plomp, G., Herzog, M. H., Michel, C. M., & De Lucia, M. (2012). Decoding stimulus-related information from single-trial EEG responses based on voltage topographies. *Pattern Recognition*, *45*(6), 2109–2122. http://dx.doi.org/10.1016/j.patcog.2011.04.007.

Uhlhaas, P. J., Pipa, G., Lima, B., Melloni, L., Neuenschwander, S., Nikolić, D., & Singer, W. (2009). Neural synchrony in cortical networks: History, concept and current status. *Frontiers in Integrative Neuroscience*, *3*(JUL), 1–19. http://dx.doi.org/10.3389/neuro.07.017.2009.

Varela, F., Lachaux, J. P., Rodriguez, E., & Martinerie, J. (2001). The brainweb: Phase synchronization and large-scale integration. *Nature Reviews Neuroscience*, *2*(4), 229–239. http://dx.doi.org/10.1038/35067550.

Varsehi, H., & Firoozabadi, S. M. P. (2021). An EEG channel selection method for motor imagery based brain–computer interface and neurofeedback using granger causality. *Neural Networks*, *133*, 193–206. http://dx.doi.org/10.1016/j.neunet.2020.11.002.

Vasicek, O. (1976). A test for normality based on sample entropy. *Journal of the Royal Statistical Society. Series B. Statistical Methodology*, *38*(1), 54–59, http://www.jstor.org/stable/2984828.

Vicente, R., Gollo, L. L., Mirasso, C. R., Fischer, I., & Pipa, G. (2008). Dynamical relaying can yield zero time lag neuronal synchrony despite long conduction delays. *Proceedings of the National Academy of Sciences of the United States of America*, *105*(44), 17157–17162. http://dx.doi.org/10.1073/pnas.0809353105.

Vidaurre, D., Hunt, L. T., Quinn, A. J., Hunt, B. A. E., Brookes, M. J., Nobre, A. C., & Woolrich, M. W. (2018). Spontaneous cortical activity transiently organises into frequency specific phase-coupling networks. *Nature Communications*, *9*(1), http://dx.doi.org/10.1038/s41467-018-05316-z.

Von Bünau, P., Meinecke, F. C., Király, F. C., & Müller, K. R. (2009). Finding stationary subspaces in multivariate time series. *Physical Review Letters*, *103*(21), Article 214101. http://dx.doi.org/10.1103/PhysRevLett.103.214101.

Walden, A. T., & Contreras Cristan, A. (1998). The phase-corrected undecimated discrete wavelet packet transform and its application to interpreting the timing of events. *Proceedings of the Royal Society A: Mathematical, Physical and Engineering Sciences*, *454*(1976), 2243–2266. http://dx.doi.org/10.1098/rspa.1998.0257.

Wang, H. E., Bénar, C. G., Quilichini, P. P., Friston, K. J., Jirsa, V. K., & Bernard, C. (2014). A systematic framework for functional connectivity measures. *Frontiers in Neuroscience*, *8*(DEC), 405. http://dx.doi.org/10.3389/fnins.2014.00405.

Wang, J., Feng, Z., Lu, N., & Luo, J. (2018). Toward optimal feature and time segment selection by divergence method for EEG signals classification. *Computers in Biology and Medicine*, *97*, 161–170. http://dx.doi.org/10.1016/j.compbiomed.2018.04.022.

Wang, J., Feng, Z., Ren, X., Lu, N., Luo, J., & Sun, L. (2020). Feature subset and time segment selection for the classification of EEG data based motor imagery. *Biomedical Signal Processing and Control*, 61. http://dx.doi.org/10.1016/j.bspc.2020.102026.

Wang, Yijun, Hong, B., Gao, X., & Gao, S. (2006). Phase synchrony measurement in motor cortex for classifying single-trial EEG during motor imagery. In *Annual international conference of the ieee engineering in medicine and biology - proceedings* (pp. 75–78). http://dx.doi.org/10.1109/IEMBS.2006.259673.

Wang, Yifeng, Huang, X., Yang, X., Yang, Q., Wang, X., Northoff, G., Pang, Y., Wang, C., Cui, Q., & Chen, H. (2019). Low frequency phase-locking of brain signals contribute to efficient face recognition. *Neuroscience*, *422*, 172–183. http://dx.doi.org/10.1016/j.neuroscience.2019.10.024.

Wei, Q., Wang, Y., Gao, X., & Gao, S. (2007). Amplitude and phase coupling measures for feature extraction in an EEG-based brain-computer interface. *Journal of Neural Engineering*, *4*(2), 120–129. http://dx.doi.org/10.1088/1741-2560/4/2/012.

Wendling, F., Ansari-Asl, K., Bartolomei, F., & Senhadji, L. (2009). From EEG signals to brain connectivity: A model-based evaluation of interdependence measures. *Journal of Neuroscience Methods*, *183*(1), 9–18. http://dx.doi.org/10.1016/j.jneumeth.2009.04.021.

Wibral, M., Pampu, N., Priesemann, V., Siebenhühner, F., Seiwert, H., Lindner, M., Lizier, J. T., & Vicente, R. (2013). Measuring information-transfer delays. *PLoS One*, *8*(2), Article e55809. http://dx.doi.org/10.1371/journal.pone.0055809.

Wibral, M., Rahm, B., Rieder, M., Lindner, M., Vicente, R., & Kaiser, J. (2011). Transfer entropy in magnetoencephalographic data: Quantifying information flow in cortical and cerebellar networks. *Progress in Biophysics & Molecular Biology*, *105*(1–2), 80–97. http://dx.doi.org/10.1016/j.pbiomolbio.2010.11.006.

Wibral, M., Vicente, R., & Lindner, M. (2014). Transfer entropy in neuroscience. (pp. 3–36). http://dx.doi.org/10.1007/978-3-642-54474-3_1.

Wierzgała, P., Zapała, D., Wojcik, G. M., & Masiak, J. (2018). Most popular signal processing methods in motor-imagery BCI: A review and meta-analysis. *Frontiers in Neuroinformatics*, *12*(78), http://dx.doi.org/10.3389/fninf.2018.00078.

Witham, C. L., Wang, M., & Baker, S. N. (2007). Cells in somatosensory areas show synchrony with beta oscillations in monkey motor cortex. *European Journal of Neuroscience*, *26*(9), 2677–2686. http://dx.doi.org/10.1111/j.1460-9568.2007.05890.x.

Wolpaw, J. R., Birbaumer, N., McFarland, D. J., Pfurtscheller, G., & Vaughan, T. M. (2002). Brain-computer interfaces for communication and control. *Clinical Neurophysiology*, *113*(6), 767–791. http://dx.doi.org/10.1016/S1388-2457(02)00057-3.

Xie, H., Calhoun, V. D., Gonzalez-Castillo, J., Damaraju, E., Miller, R., Bandettini, P. A., & Mitra, S. (2018). Whole-brain connectivity dynamics reflect both task-specific and individual-specific modulation: A multitask study. In *NeuroImage, Vol. 180* (pp. 495–504). Academic Press Inc, http://dx.doi.org/10.1016/j.neuroimage.2017.05.050.

Xu, J. W., Bakardjian, H., Cichocki, A., & Principe, J. C. (2008). A new nonlinear similarity measure for multichannel signals. *Neural Networks*, *21*(2–3), 222–231. http://dx.doi.org/10.1016/j.neunet.2007.12.039.

Xu, L., Zhang, H., Hui, M., Long, Z., Jin, Z., Liu, Y., & Yao, L. (2014). Motor execution and motor imagery: A comparison of functional connectivity patterns based on graph theory. *Neuroscience*, *261*, 184–194. http://dx.doi.org/10.1016/j.neuroscience.2013.12.005.

Yuan, H., & He, B. (2014). Brain-computer interfaces using sensorimotor rhythms: Current state and future perspectives. *IEEE Transactions on Biomedical Engineering*, *61*(5), 1425–1435. http://dx.doi.org/10.1109/TBME.2014.2312397, IEEE Computer Society.

Zalesky, A., Fornito, A., & Bullmore, E. (2012). On the use of correlation as a measure of network connectivity. *NeuroImage*, *60*(4), 2096–2106. http://dx.doi.org/10.1016/j.neuroimage.2012.02.001.

Zalesky, A., Fornito, A., Cocchi, L., Gollo, L. L., & Breakspear, M. (2014). Time-resolved resting-state brain networks. *Proceedings of the National Academy of Sciences of the United States of America*, *111*(28), 10341–10346. http://dx.doi.org/10.1073/pnas.1400181111.

Zanon, M., Borgomaneri, S., & Avenanti, A. (2018). Action-related dynamic changes in inferior frontal cortex effective connectivity: A TMS/EEG coregistration study. *Cortex*, *108*, 193–209. http://dx.doi.org/10.1016/j.cortex.2018.08.004.

Zhang, Y., Nam, C. S., Zhou, G., Jin, J., Wang, X., & Cichocki, A. (2019). Temporally constrained sparse group spatial patterns for motor imagery BCI. *IEEE Transactions on Cybernetics*, *49*(9), 3322–3332. http://dx.doi.org/10.1109/TCYB.2018.2841847.

Zhang, Y., Zhou, G., Jin, J., Wang, X., & Cichocki, A. (2015). Optimizing spatial patterns with sparse filter bands for motor-imagery based brain-computer interface. *Journal of Neuroscience Methods*, *255*, 85–91. http://dx.doi.org/10.1016/j.jneumeth.2015.08.004.

Zink, N., Mückschel, M., & Beste, C. (2020). Resting-state EEG dynamics reveals differences in network organization and its fluctuation between frequency bands. *Neuroscience*, *453*, 43–56. http://dx.doi.org/10.1016/j.neuroscience.2020.11.037.

Ziqiang, Z., & Puthusserypady, S. (2007). Analysis of schizophrenic EEG synchrony using empirical mode decomposition. In *2007 15th international conference on digital signal processing, DSP 2007* (pp. 131–134). http://dx.doi.org/10.1109/ICDSP.2007.4288536.